Adenosine A1 Receptor Ligands Bind to α-Synuclein: Implications for α-Synuclein Misfolding and α-Synucleinopathy in Parkinson's Disease

Elisabet Jakova
University of Saskatchewan College of Medicine
Mohamed Taha Moutaoufik
University of Regina
Jeremy Lee
University of Saskatchewan College of Medicine
Mohan Babu
University of Regina Faculty of Science
Francisco Sandoval Cayabyab (frank.cayabyab@usask.ca)
University of Saskatchewan College of Medicine https://orcid.org/0000-0002-5058-7087

Research

Keywords: Alpha-Synucleinopathy, adenosine A1 receptor, N6-Cyclopentyladenosine, 8-Cyclopentyl-1, 3-dipropylxanthine, 1-aminoindan, 2-aminoindan, neurodegeneration, Parkinson's disease, molecular dynamics simulation, nanopore analysis

Posted Date: December 16th, 2020

DOI: https://doi.org/10.21203/rs.3.rs-125972/v1

Version of Record: A version of this preprint was published at Translational Neurodegeneration on February 10th, 2022. See the published version at https://doi.org/10.1186/s40035-022-00284-3.

Abstract

Background:

Accumulating α-synuclein (α-Syn) aggregates in neurons and glial cells are the staples of many synucleinopathy disorders, such as Parkinson's disease. Since brain adenosine becomes greatly elevated in ageing brains and chronic adenosine A1 receptor (A1R) stimulation leads to neurodegeneration, we determined whether adenosine or A1R receptor ligands mimic the action of known compounds that promote α-Syn aggregation (e.g., the amphetamine analogue 2-aminoindan) or inhibit α-Syn aggregation (e.g., Rasagiline metabolite 1-aminoindan). In the present study, we determined whether adenosine, the A1R receptor agonist N^6-Cyclopentyladenosine (CPA) and antagonist 8-Cyclopentyl-1,3-dipropylxanthine (DPCPX) directly interact with α-Syn to modulate α-Syn aggregation and neurodegeneration of dopaminergic neurons in the substantia nigra (SN).

Methods:

Nanopore analysis and molecular dynamics simulation were used to test the binding properties of CPA and DPCPX with α-Syn *in vitro*. Sprague-Dawley rats were administered 7-day intraperitoneal injections of the A1R ligands and 1- and 2-aminoindan, and levels of α-Syn aggregation and neurodegeneration were examined in the substantia nigra *pars compacta* region.

Results:

Using nanopore analysis, we showed that the A1R agonists (CPA and adenosine) interacted with the N-terminus of α-Syn, similar to 2-aminoindan, which is expected to promote a "knot" conformation and α-Syn misfolding. In contrast, the A1R antagonist DPCPX interacted with the N- and C-termini of α-Syn, similar to 1-aminoindan, which is expected to promote a "loop" conformation which prevents α-Syn misfolding. Molecular docking studies revealed that adenosine, CPA and 2-aminoindan interacted with the hydrophobic core of α-Syn N-terminus, whereas DPCPX and 1-aminoindan showed direct binding to the N- and C-terminal hydrophobic pockets. Histological and confocal imaging studies revealed that chronic treatments with CPA alone or in combination with 2-aminoindan increased α-Syn aggregation and neurodegeneration in SN *pars compacta*. In contrast, DPCPX and 1-aminoindan attenuated CPA-induced neurodegeneration but did not significantly reduce α-Syn aggregation.

Conclusions:

The results indicate A1R agonists and drugs promoting a "knot" conformation of α-Syn can cause α-synucleinopathy and increase neuronal degeneration, whereas A1R antagonists and drugs promoting a "loop" conformation of α-Syn can be harnessed for possible neuroprotective therapies to decrease α-synucleinopathy in Parkinson's disease.

Background

Adenosine is a nucleoside that is involved in many physiological activities including cell proliferation, migration of dendritic cells, and the release of small proteins called cytokines which are vital for cell signalling from periphery to secondary lymphoid organs, vascular reactivity, apoptosis and most importantly in the passage of neuronal stem cells [1–5]. Adenosine is also implicated in central nervous system (CNS) disorders such as ischemia, trauma, epilepsy, neuropsychiatric disorders and cancer [6–11]. Moreover, various roles of adenosine have garnered intense investigations in many ageing-related neurodegenerative diseases such as ischemic stroke, Alzheimer disease (AD) and Parkinson's disease (PD) [12–15]. PD is the second most prevalent ageing-related neurodegenerative disease after AD [16]. The pathophysiology of PD directly involves the imbalance of dopaminergic signalling pathways and accumulation of protein aggregates of α-Synuclein (α-Syn) in inclusions (Lewy bodies) causing the characteristic motor and cognitive deficits commonly observed in PD patients [17–19]. Recently, some neuroprotective drugs have been found to bind to α-Syn and prevent further aggregation, including caffeine, nicotine, 1-aminoindan and metformin [20]. Additionally, there are other drugs such as methamphetamine, cocaine, 2-aminoindan and the herbicides, paraquat and rotenone, which appear to be neurotoxic because they increase α-Syn misfolding and can be correlated with a higher incidence of PD [20–23]. Chronic adenosine A1 receptor (A1R) stimulation has recently been reported to cause hippocampal and substantia nigra (SN) neuronal death, as well as increased α-Syn accumulation in dopaminergic SN neurons [24, 25]. Since a primary therapeutic goal of management of PD is to minimize α-Syn misfolding and aggregation, we investigated whether adenosine and the A1R agonist N^6-Cyclopentyladenosine (CPA) and antagonist 8-Cyclopentyl-1,3-dipropylxanthine (DPCPX) bind to and modulate α-Syn misfolding.

A1Rs are expressed at high levels in the limbic system especially in the hippocampus as well as in the SN region. A1R stimulation with CPA reduced glutamate and GABA release from nerve terminals of the SN pars reticulata region of the rat brain [26]. This presynaptic inhibition of glutamate release from the subthalamonigral pathway may be clinically relevant in improving tardive dyskinesia in PD patients by reducing the glutamatergic outputs of the SN pars reticulata dopaminergic neurons. Moreover, most compounds that target A1R activation were believed to be neuroprotective in both the SN and hippocampus. For example, activation of A1R is involved in paeoniflorin (a chemical compound derived from Paenoia lactiflora)-induced neuroprotection in cerebral ischemia in Sprague-Dawley rats [27]. However, we recently reported that chronic stimulation of A1Rs by intraperitoneal (i.p.) injection of rats for 3 days with the A1R agonist CPA was sufficient to induce neurodegeneration in the hippocampus [24]. Additionally, longer-term 5-week chronic A1R stimulation with CPA increased sortilin expression that promoted α-Syn upregulation in dopaminergic MN9D cells and SN dopaminergic neurons of Sprague-Dawley rats [25]. Since highly upregulated α-Syn and A1R can be found in the hippocampus and SN of rodent synucleinopathy models, we therefore tested the possibility that the commonly used A1R-selective agonist ligand CPA can bind to α-Syn and enhance neurotoxicity, whereas the A1R-specific antagonist ligand DPCPX can bind to α-Syn and promote neuroprotection [28–30]. Here, we established a 7-day chronic injections model using Sprague-Dawley male rats to determine if indeed chronic stimulation with CPA causes dopaminergic neuron loss as well as increased expression of α-Syn in SN. We then co-

administrated DPCPX as a method to control neurodegeneration and decrease aggregation of α-Syn caused initially by CPA. Staining like Fluoro-Jade C (FJC) and Thioflavin S (ThioS) were used to assess neurodegeneration and α-Syn aggregation respectively [31, 32].

Nanopore analysis and molecular dynamic simulations are useful analytical tools for studying intrinsically disordered proteins like α-Syn. Nanopores are single-molecule counters consisting of a nanometre aperture that allows the fluxes of ions and small charged polypeptides through an insulating membrane. Applying a voltage across this membrane results in an electrochemical gradient that drives ions through the α-hemolysin (α-HML) toxin derived from Staphylococcus aureus [33]. A single α-Syn protein interacts with the α-HML pore causing a blockade current (I) for an amount of time (T) (Fig. 1) [34]. When α-Syn translocates through the pore a large current blockade is observed for a long translocation time. Conversely, if the α-Syn protein approaches the pore but then diffuses away without entering, a small current blockade is observed for a short time. This type of event is called bumping [35, 36]. The most important advantage of nanopore analysis is that molecules can be detected without labelling and at very low concentrations. Uniquely, this technique requires less than an hour to non-destructively analyze thousands of single molecules. Additionally, molecular dynamics simulation is a computer simulation technique that allows prediction of the binding conformation of a desired protein or peptide to a chemical compound or other small molecule, making molecular docking analysis one of the best techniques for structure-based drug design [37, 38]. Therefore, using these complimentary biophysical and computational techniques, in combination with *in vivo* treatments of rats with A1R ligands and other compounds, we aimed to elucidate the effects of adenosine and other A1R ligands on α-Syn misfolding patterns and the functional consequences of these interactions *in vivo* by examining the health of the SN dopaminergic neurons that are affected in Parkinson's disease.

Methods

Animal protocol. Animals were treated with responsibility, humanity and conscientiousness accordingly following the guidelines of the followings: National Research Council (US) Committee for the Update of the Guide for the Care and Use of Laboratory Animals (Washington DC, 2011); Canadian Council on Animal Care (CCAC) and the University of Saskatchewan Lab Animal Services Unit (LASU) approved protocol. Male Sprague-Dawley rats (20–30 days old varying from 250–300 g) were used for confocal experiments. The animals were housed in cages of two where unlimited access to food pellets and water was provided by the LASU staff.

Reagents. α-Synuclein was acquired from rPeptide (Bogart, GA, USA). The protein was dissolved in Nuclease-Free water at a final concentration of 1 μM. Adenosine was purchased from Millipore-Sigma (Oakville, ON, Canada), CPA was purchased from Abcam (Toronto, ON, Canada), DPCPX from Tocris (Burlington, ON, Canada), 1- and 2-aminoindan were purchased from Sigma-Aldrich (Oakville, ON, Canada). For the nanopore analysis, all drugs were dissolved in methanol and used at a final concentration of 10 μM. For the 7-day chronic intraperitoneal injection of CPA, DPCPX, 1- and 2-

aminoindan were dissolved in 0.1% (of the 0.9% Sodium Chloride sterile final volume) dimethyl sulfoxide (DMSO) purchased from Sigma-Aldrich (Oakville, ON, Canada) at a final concentration of 3 mg/ml.

Nanopore analysis

a. Instrument setup. The standard DC setup has been described in detail previously by our lab [34, 39, 40]. In brief, a lipid bilayer was painted onto a 150 μm aperture in a Teflon perfusion cup. The two buffer compartments on either side of the lipid bilayer each contained a 1 ml total volume. Five μL of 1 μg ml^{-1} of α-hemolysin (α-HML) (Millipore-Sigma, Oakville, ON, Canada) was added to the *cis* side of the membrane and the current was monitored until stable pore insertion was achieved. Consistent results were achieved with one to four pores. The peptides were added to the cis side of the pore with the positive electrode on the trans-side. The experiments were carried out at 22 ± 1 °C with an applied potential of 100 mV at a bandwidth of 10 KHz using an Axopatch 200B amplifier (Axon Instruments, San Jose, CA, USA) under voltage clamp conditions and Clampfit software. As discussed elsewhere, temperature changes due to Joule heating are expected to be negligible.

b. Data analysis. The blockade amplitudes and duration times obtained with Clampfit were transferred to Origin 7 graphing software (OriginLab Corporation, Northampton, MA, USA) and were used to construct blockade current and time histograms. The blockade amplitudes were plotted as statistical histograms and each event population (e.g. translocation, intercalation and bumping) was fitted with a Gaussian function to obtain the peak/population blockade current value (I). The duration time data for each population was plotted separately and the data fitted with a single exponential decay function to obtain the characteristic time (T). Each experiment was repeated at least three times and the event profiles were added together. The error in the peak current was estimated to be < ± 1 pA and the proportion of the events in each peak is reported in Tables as means % ± SEM%.

c. Statistical analysis. Statistical significance of the populations and time events was determined using GraphPad Prism 8 software (San Diego, CA, USA). A one-way analysis of variance (ANOVA) followed by Student-Neuman-Keuls multiple comparison *post hoc* test was used for Tables 1 and 2. A *P*-value < 0.05 was considered statistically significant.

Table 1
Populations and the blockade times of each of translocations and bumping events for α-Syn alone and α-Syn complexes with adenosine, CPA, and DPCPX. The standard error of the mean (SEM) is calculated in percentage of events for populations and in milliseconds for blockade times. ns $p > 0.05$; * $p < 0.05$; ** $p < 0.01$; and *** $p < 0.001$.

Protein - Drug complex	α-Syn	α-Syn + Adenosine	α-Syn + CPA	α-Syn + DPCPX
Population of Translocation	66%	52% [*]	40% [**]	37% [**]
SEM	1%	2%	1%	1%
Population of Bumping	24%	25% [ns]	37% [**]	46% [**]
SEM	1%	3%	2%	2%
Time of Translocation	0.52 ms	0.46 ms [ns]	0.47 ms [ns]	0.42 ms [ns]
SEM	0.05 ms	0.05 ms	0.05 ms	0.04 ms
Time of Bumping	0.05 ms	0.12 ms [ns]	0.09 ms [ns]	0.07 ms [ns]
SEM	< 0.01 ms	0.01 ms	< 0.01 ms	< 0.01 ms

Table 2
Summary of the intensity and the population of the current blockades for all the domains with or without CPA or DPCPX. The standard error of the mean is calculated in picoamps for the intensities and percentage of events for populations (I and P stands for intensity and population of the current blockade respectively). ns $p > 0.05$; * $p < 0.05$; ** $p < 0.01$; and *** $p < 0.001$.

Domain - Drug complex	I_{Trans}	P_{Trans}	I_{Inter}	P_{Inter}	I_{Bump}	P_{Bump}
N-term	-	-	-	-	-30 pA ± 1 pA	70% ± 2%
N-term + CPA	-66 pA ± 6 pA	35% ± 3%	-	-	-26 pA ± 1 pA	46% ± 2% [***]
N-term + DPCPX	-72 pA ± 7 pA	36% ± 10%	-51 pA ± 2 pA	21% ± 12%	-30 pA ± 2 pA	41% ± 1% [***]
C-term	-69 pA ± 2 pA	77% ± 4%	-	-	-30 pA ± 2 pA	20% ± 3%
C-term + CPA	-66 pA ± 3 pA	70% ± 8% [ns]	-	-	-38 pA ± 4 pA	23% ± 3% [ns]
C-term + DPCPX	-64 pA ± 1 pA	38% ± 2% [***]	-31 pA ± 1 pA	33% ± 4%	-19 pA ± 1 pA	7% ± 1% [ns]
ΔNAC	-86 pA ± 2 pA	58% ± 2%	-	-	-27 pA ± 1 pA	19% ± 4%
ΔNAC + CPA	-	-	-36 pA ± 3 pA	66% ± 3%	-	-
ΔNAC + DPCPX	-	-	-39 pA ± 1 pA	35% ± 5%	-24 pA ± 2 pA	34% ± 3%

Structural Modeling and Docking. *de novo* protein trRosetta was used to predict the unresolved structure of α-Syn [41]. α-Synuclein crystal structure is not yet known, however, several nuclear magnetic resonance (NMR) and homology modeled structures are available from protein data bank. The 1XQ8 Human micelle-bound α-Synuclein structure and homology modeled structure were used in this manuscript [42]. The chemical structure of Adenosine, CPA, DPCPX, 1-aminoindan and 2-aminoindan were obtained from PubChem (CIDs: 60961, 53477947, 1329, 123445, 76310), respectively. The molecular docking study was carried out using Autodock Vina module implemented in PyRx tool [38]. Protein and ligand interactions were analyzed and visualized through Pymol and LigPlot+.

In vivo **drug treatments to study alpha synuclein aggregation and neurodegeneration.**

In support of the *in vitro* data, a full *in vivo* study consisting of a 7-day chronic intraperitoneal (i.p.) injections of 28-day old male Sprague Dawley rats was performed. The eight treatments consist of **1.** Control (0.1% DMSO in 0.9% saline), **2.** CPA, **3.** DPCPX, **4.** 1-aminoindan, **5.** 2-aminoindan, **6.** CPA + DPCPX, **7.** 1-aminoindan + CPA, and **8.** 2-aminoindan + CPA. Although 1-aminoindan and 2-aminoindan have a very similar structure they have shown to possess very different properties *in vitro*, therefore we suggest they will exhibit different physiological properties *in vivo* as well. All drugs were dissolved at 3 mg/ml in DMSO, and each drug was administered to the animals by daily i.p. injections (3 mg/kg body weight) for 7 consecutive days. After the first injections with DPCPX, 1- or 2-aminoindan a waiting period of 30 minutes was applied before administrating the CPA injection. Then on the eighth day following the final injections, the animals were sacrificed and prepared for brain immunohistochemistry and confocal imaging as described below.

Immunohistochemistry. Anesthetized rats were transcardially perfused with 0.9% saline then fixed with 4% paraformaldehyde. The extracted brains were then put in 30% cryoprotected sucrose solution for 48 hrs prior to slicing. The brains were initially frozen at -40 °C (BFS-30 mp controllers) and sliced with the help of microtome (Leica SM2010 R Sliding controller). Coronal slices of 40 µm were then washed three times in 0.1M phosphate buffered saline followed by 1 hr blocking at room temperature with blocking buffer. The solution recipe and detailed recordings were previously described [43]. The slices were then incubated overnight at 4 °C with the following primary antibodies: 1:200 mouse monoclonal to α-Synuclein (Abcam Inc, Toronto, ON, Canada) and 1:200 rabbit polyclonal to Tyrosine Hydroxylase (Millipore-Sigma, Oakville, ON, Canada). Subsequently, slices were then incubated for 1 hour in the dark at room temperature with the following secondary antibodies: AlexaFluor-555-conjugated anti-mouse and AlexaFluor-647-conjugated anti-rabbit (1:1000) purchased from Invitrogen (Thermo Fisher Scientific, Waltham, MA, USA). Slices were then treated with Thioflavin-S (The solution recipe and detailed recordings are described below). Lastly, the slices were incubated for 5 minutes at room temperature with DAPI (2 mg/ml) from Invitrogen (Thermo Fisher Scientific, Waltham, MA, USA) and images were taken using a Zeiss LSM700 confocal microscope (Carl Zeiss Group, Canada) and analyzed with ImageJ (Public Domain).

Thioflavin-S. Thioflavin-S (Sigma-Aldrich, Oakville, ON, Canada) is a fluorescent marker used to detect α-Synuclein aggregates and amyloid plaques. After performing the immunohistochemistry, coronal slices of 40 µm were firstly treated with 0.3% $KMnO_4$ for 4 minutes, followed by a 30-min incubation with 1M phosphate buffered saline at 4 °C. These slices were then stained with 0.05% Thioflavin-S in 50% Ethanol in the dark for 8 minutes. Slices were then rinsed with 80% Ethanol twice followed by three rinses with ultra-pure water for 30 seconds. Slices were then finally incubated again with 1M phosphate buffered saline for 30 minutes at 4 °C before starting the DAPI stain. The FITC filter (488 nm laser line) was used to image Thioflavin-S using a Zeiss LSM700 confocal microscope (Carl Zeiss Group, Canada) and analyzed with ImageJ (Public Domain).

Fluoro-Jade C. This stain is a fluorescent marker for neurodegeneration (Millipore-Sigma, Oakville, ON, Canada). Coronal slices of 40 µm were mounted on 5% gelatin coated super-frost plus microscope slides

(Thermo Fisher Scientific, Waltham, MA, USA) and dried overnight at 4 °C. Initially, the microscope slides were immersed in 1% NaOH/80% Ethanol for 5 minutes followed by 2 minutes immersion in 70% Ethanol. The slides were then rinsed for 2 minutes with ultra-pure water. The microscope slides were further immersed in 0.06% $KMnO_4$ for 10 minutes, followed by additional rinse for 2 minutes with ultra-pure water. The slides were then stained with 0.004% Fluoro-Jade C in 0.1% Acetic acid for 20 minutes with gentle shaking on an orbital shaker. Lastly, the slides were rinsed three times in ultra-pure water for 1 minute each making sure to remove all the excess water after each rinse. Slides were then rinsed in xylene and allowed to dry overnight at 4 °C. Slides were treated with Prolong Gold Antifade Reagent from Invitrogen (Thermo Fisher Scientific, Waltham, MA, USA) and respective images were taken using a Zeiss LSM700 confocal microscope (Carl Zeiss Group, Canada) and analyzed with ImageJ (Public Domain). Fluoro-Jade C fluorescence was obtained by exciting the dye with 488 nm laser.

Histological statistical analyses. All post-mortem statistical analysis was conducted with GraphPad Prism 8 software (San Diego, CA, USA) with one-way ANOVA followed by multiple comparisons using Student-Neuman-Keuls *post hoc* test. A *P*-value < 0.05 was considered statistically significant.

Results

CPA and DPCPX bind to Alpha-Synuclein in vitro.

Initially, both CPA and DPCPX were tested by nanopore analysis. Once a stable pore was created, a final concentration of 1 μM α-Syn was inserted on the *cis* side of the perfusion cup. At first, a few bumping events at 30 pA and a higher number of translocation events around 85 pA were observed, whereas intercalation events (I) were rarely encountered, as shown in Fig. 1b.2. Thus, these observations confirm similar recordings of stable blockade and bumping currents of α-Syn, as previously reported [33]. Then, 10 μM final drug concentration was inserted on the *cis* side and possible changes of blockade events could be observed.

First, we tested the potential binding of adenosine with α-Syn in our nanopore setup. As shown in Fig. 2b, adenosine appears to have weak binding affinity to α-Syn. The majority of the events of the − 86 pA blockade current are related to α-Syn translocation; however, there are fewer events observed in the translocation peak in the α-Syn and adenosine histogram (52%) in comparison to α-Syn alone (66%). Interestingly, CPA and DPCPX appear to bind to α-Syn as well, as shown in Fig. 2c and d. For the first time, we observed a decrease in the blockade current of the translocation peak from − 85 pA for α-Syn alone to -89 pA for the α-Syn and CPA complex (Fig. 2c), as the percentage of events decreased from 66–40% for CPA. Taken together the observed effects of CPA and, to a lesser extent, adenosine on the α-Syn translocation events are clear signs of binding. Conversely, DPCPX caused a small increase of the blockade current to -84 pA which was accompanied by a decrease of the number of events in the translocation peak (Fig. 2d). The blockade times of translocation and bumping peaks of α-Syn with and without adenosine, CPA and DPCPX were calculated. Representative exponential time graphs are shown in Fig. 3. The times of translocation and bumping events for α-Syn alone are well established [33]. The

times of translocation events (α-Syn alone, 0.52 ms) decrease when α-Syn was combined with adenosine (0.46 ms), CPA (0.47 ms) or DPCPX (0.42 ms), which further indicates a potential binding of these drugs to the protein. On the other hand, we observed increased bumping times when α-Syn was incubated with adenosine, CPA or DPCPX (see Fig. 3e-h). A full summary of the blockade populations and times is shown in Table 1.

Caffeine, a nonselective inhibitor of all the adenosine receptors (A1, A2A, A2B and A3) [44], has been previously studied with nanopore analysis and it showed binding to the N- and C-terminus forming a neuroprotective loop conformation [40]. It is known that caffeine competitively antagonizes adenosine's effect [45, 46]. Although the blockade populations of adenosine and CPA show some similarities to the histogram of caffeine binding to α-Syn [47], however, both adenosine and CPA decrease the blockade current of the translocation events of α-Syn to -86 and − 89 pA, respectively (see Fig. 2b and c). Previous results using 5 μM caffeine showed that the translocation population decreased to 44% from 81% of α-Syn alone, whereas the bumping population significantly increased to 38% compared to 9% of α-Syn alone [47]. This is similar to the decrease of the translocation population (37%) and increase of the bumping population (46%) observed with DPCPX + α-Syn (see Fig. 2d). Therefore, similar to caffeine, DPCPX potentially binds to the N- and C-termini of α-Syn forming a loop conformation. Further probing of the exact binding of both CPA and DPCPX was conducted using separate domains of α-Syn.

Alpha-Synuclein domain investigations of CPA and DPCPX

The two domains of α-Syn, namely the N- and C-termini, and the ΔNAC construct consisting of α-Syn with deleted non-Amyloidβ-component region (see Fig. 1d and e) were tested against CPA or DPCPX. The behaviour of each domain is different in a standard nanopore analysis at a direct current voltage of 100 mV (Fig. 4a, d, g). The blockade current histogram of the N-terminus has a single Gaussian peak at -30 pA due to bumping events. The N-terminus is positively charged (+ 4). Consequently, it will be difficult for this N-terminal fragment to translocate through the pore under the applied positive transmembrane voltage. Conversely, the C-terminus contains a total of 12 negative charges which permits translocation through the pore. The blockade current histogram has a large and wide translocation peak at -69 pA and a fairly small bumping peak at -30 pA. The ΔNAC has two peaks, a large peak at -86 pA due to translocation and a smaller one at -27 pA due to bumping.

In Fig. 4 are shown the blockade current histograms of each α-Syn domain in presence of CPA (Fig. 4b, e, h) and DPCPX (Fig. 4c, f, i). With the addition of CPA, the N-terminus proportion of bumping events decreased significantly from 70–46% (Fig. 4a vs. b). Conversely, the widespread block of events between − 50 and − 100 pA in the N-terminus control developed into a well-defined broad translocation peak at -26 pA with a population of 35%. The changes observed in the ΔNAC after the addition of CPA are remarkable and demonstrate clear signs of binding (Fig. 4d vs. e). The broad translocation peak at -86 pA has been reduced into a small cluster of events, whereas the small bumping peak significantly increased in population from 19–66% and has shifted to -36 pA from − 27pA. Interestingly, the C-terminal domain

histogram profiles in absence and presence of CPA did not show significant differences (Fig. 4g vs. h), which indicates that CPA does not interact with the C-terminus.

In contrast, DPCPX produced different profile histograms of each of the α-Syn domains when compared to both the control and CPA. The N-terminus histogram profile shows that DPCPX caused a decrease in the proportion of bumping events from 70–41%, and DPCPX also revealed two additional peaks, namely the translocation peak at -72 pA and an intercalation peak at -51 pA (Fig. 4a vs. c). The intercalation peak at -51 pA has a low population of events (21%) whereas the translocation peak is broader and has a similar proportion to the translocation peak of CPA. The ΔNAC translocation peak disappears with the addition of DPCPX; instead, two peaks with similar proportion of events are observed at -24 and − 39 pA, representing the bumping and intercalation peaks, respectively (Fig. 4d vs. f). Lastly, the C-terminus histogram of DPCPX indicates a decrease of the bumping events from 20–7%, an emergence of an intercalation peak at -31 pA, and a significant decrease of the translocation peak from 77–38% (Fig. 4g vs. i). For convenience, all the blockade intensities and populations events are shown in Table 2.

Molecular dynamics simulations reveal CPA, adenosine and 2-aminoindan bind to the N-terminus of Alpha-Synuclein.

In order to confirm our biophysical results obtained from nanopore analysis, we further characterized the α-Syn-drug complexes by performing molecular docking attempts of the three A1R ligands as well as 1- and 2-aminoindan with α-Syn. Based on the nanopore analysis, a simulation of adenosine, A1R agonist CPA and methamphetamine analog 2-aminoindan was conducted (Fig. 5). As α-Syn crystal structure is still unknown, the 1XQ8 micelle-bound human α-Syn structure was used [42]. As shown in Fig. 5, adenosine, CPA and 2-aminoindan all bind to the same region of the N-terminus of α-Syn (blue alpha-helix region). As seen in Fig. 5a, adenosine forms hydrogen bonds with the lysine 32 (K32) and lysine 43 (K43) in the positively charged cleft of the α-Syn N-terminus. Adenosine forms additional hydrogen bonds with negatively charged glutamic acid 35 (E35) and interacts with the aromatic hydrophobic tyrosine 39 (Y39) and valine 40 (V40). CPA is a chemical derivative of adenosine and shows greater selectivity as A1R agonist, and thus it is expected to interact with α-Syn similarly to adenosine. As shown in Fig. 5b, CPA interacts with similar positively charged cleft containing K32 and K43 and forms additional bonds with E35. However, CPA further interacts with the polar uncharged threonine 33 (T33) and with the hydrophobic alanine 29 (A29) and V40. Lastly, 2-aminoindan is also shown to form hydrogen bonds with the negatively charged E35 (Fig. 5c), which is in common with adenosine and CPA. Moreover, as with adenosine and CPA docking simulations, 2-aminoindan also interacts with V40 and K43.

DPCPX and 1-aminoindan show interactions with Alpha-Synuclein N- and C-termini from molecular dynamics simulations.

In contrast with adenosine, CPA and 2-aminoindan, the A1R antagonist DPCPX and Rasagiline metabolite 1-aminoindan appear to possess a more intricate binding interactions with α-Syn. For these simulations both the 1XQ8 micelle-bound human α-Syn and the homology modeled structures were used. As seen in the first panel of Fig. 6, DPCPX binds to the α-Syn N-terminus (amino acids K10, A11 and V13) and the

end of the NAC region (amino acids K80, T81, A85, S87 and isoleucine 88 (I88)) using the homology modeled structure (Fig. 6a), but it binds only to the distal region of the α-Syn C-terminus when the 1XQ8 structure is used (Fig. 6b). Similarly, 1-aminoindan binds to the N-terminus (amino acids phenylalanine 4 (F4) and leucine 8 (L8)) and NAC region (amino acids T81, A85 and I88) with the homology modeled structure (Fig. 6c), but it appears to bind only to the α-Syn C-terminus using the 1XQ8 model (Fig. 6d). As the full crystal structure of α-Syn is not yet available, we suggest that using the two conformations of the 1XQ8 structure and the homology modeled structure of α-Syn in our molecular docking attempts should give a more complete information of the binding interactions of DPCPX and 1-aminoindan with α-Syn. Taken together, the molecular docking studies appear to confirm the results obtained from nanopore analyses, namely that adenosine, CPA and 2-aminoindan only interacted with the α-Syn N-terminus; this is expected to promote α-Syn conformation that promotes α-Syn aggregation. In contrast, DPCPX and 1-aminoindan showed binding to both N- and C-terminal regions of α-Syn; this binding pattern is expected to promote an α-Syn conformation that prevents α-Syn aggregation.

Adenosine A1 receptor agonist and drugs that bind to α-Syn N-terminus increased α-Syn expression and aggregation in substantia nigral neurons.

To investigate whether drug binding to the N- and/or C-terminus of α-Syn can affect the levels of α-Syn expression and aggregation *in vivo*, we administered the drugs individually or in combination with the A1R agonist CPA. Our results show that 7-day systemic administration of CPA, alone or in combination with 2-aminoindan, leads to increased expression and aggregation of α-Syn in the SN *pars compacta* (Figs. 7,8). Figure 7a shows a low magnification of the whole SN stained with 3,3'Diaminobenzidine (DAB)-tyrosine hydroxylase (TH), indicating the locations of the dopaminergic neurons in the SN [48] especially in the *pars compacta* region (square box) used for subsequent quantification of α-Syn and aggregation levels (Fig. 7b, Fig. 8) and neurodegeneration levels (Fig. 9). We focused on the SN *pars compacta* region of the midbrain which is linked to PD, as the pathology of this disease is characterized by significant loss of dopaminergic neurons in this region [49, 50]. Subsequently, fixed coronal slices of 40 μm of SN were probed for TH (a marker for dopaminergic neurons), α-Syn and Thioflavin-S (Thio-S), a fluorescent stain for α-Syn aggregates and amyloids. The slices were also labelled with DAPI (fluorescent stain that binds to adenine-thymine regions in DNA) to detect cell nuclei. Confocal images were taken with 63X oil immersion objective lens at high magnification (Zeiss microscopy). Representative images of the *pars compacta* region labelled with DAPI (first column), TH (second column), and α-Syn (third column) show that α-Syn is localized in the somas (cytosol, nuclei) and presumably the dendrites of dopaminergic neurons (Fig. 7b). Interestingly, α-Syn expression was increased by CPA in absence or presence of DPCPX, 1-aminoindan, or 2-aminoindan (Fig. 7b, Fig. 8a-b) compared to the control (1% DMSO in 9% saline). The 2-aminoindan + CPA treatment induced the highest levels of the α-Syn protein expression (Fig. 8a,b). In contrast, treatments of animals with DPCPX, 1-aminoindan or 2-aminoindan alone did not significantly increase α-Syn protein expression.

To determine whether these changes in α-Syn protein expression correlated with the levels of α-Syn aggregation, the SN *pars compacta* was co-labelled with α-Syn marker and Thio-S. As shown in Fig. 8a-c,

treatments with CPA, DPCPX + CPA, 1-aminoindan + CPA, and 2-aminoindan + CPA all increased Thio-S levels. Treatment with 2-aminoindan alone also enhanced Thio-S labelling, and co-administration of 2-aminoindan with CPA caused a significant further elevation of Thio-S compared to 2-aminoindan treatment. In contrast, treatments with DPCPX and 1-aminoindan alone did not significantly increase Thio-S labelling and also did not significantly attenuate the CPA-induced increase in Thio-S levels. The colocalization of Thio-S signal with α-Syn was increased in all the treatments compared to control (about 2-fold increase in Pearson correlation coefficients, Fig. 8c). Together, these results suggest that 7-day chronic treatments with compounds that bind to the N-terminus of α-Syn (e.g., the A1R agonist CPA, 2-aminoindan) significantly increased α-Syn accumulation and aggregation.

CPA and 2-aminoindan increase neurodegeneration of SN pars compacta **dopaminergic neurons.**

Having shown that CPA and 2-aminoindan alone or in combination can increase α-Syn aggregation, we then determined whether these treatments could lead to neuronal damage. Hence, we used the FluoroJade C (FJC) as a common fluorescent marker for neurodegeneration in the CNS [31]. FJC staining was performed in nigral slices from − 5.30 to -5.60 bregma intervals. Figure 9a panels showing high magnification images of FJC staining in the *pars compacta* region of SN indicate that CPA alone, 2-aminoindan alone, and 2-aminoindan + CPA co-administration all increased the levels of FJC fluorescence (as summarized in Fig. 9b). In contrast, DPCPX or 1-aminoindan alone did not significantly increase FJC staining, but both drugs were effective in attenuating CPA-induced increase in neurodegeneration (summarized in Fig. 9b). Taken together with the above results from nanopore analysis, molecular docking and Thio-S labelling, these results suggest that compounds that bind to both N- and C-termini of α-Syn (e.g., DPCPX and 1-aminoindan) may be effective in attenuating the neurotoxic effects of compounds that bind to and promote α-Syn accumulation and misfolding (e.g., CPA, adenosine, and 2-aminoindan).

Discussion

One of the most commonly used treatments for PD patients is Levodopa (L-Dopa, a dopamine precursor). However, this treatment is associated with numerous adverse side effects such as early loss of voluntary movement, severe dyskinesia episodes and most predominantly end-of-dose worsening [51, 52]. Previous studies focused on treatments targeting dopamine receptor agonist, catechol-O-methyltransferase antagonists, monoamine oxidase inhibitors, and antagonist of dopamine transporters which show promising results in slowing the progression and alleviating the symptoms of the disease [53–56]. However, these therapies are unable to prevent PD progression without causing other significant side effects including an increased risk of cardiac-valve regurgitation, hypertension, confusion and hallucinations [57].

Adenosine binds to its inhibitory A1Rs (coupled to $G_{\alpha i}$) and its excitatory A2A receptors (A2AR, coupled to $G_{\alpha s}$), and A2ARs are believed to contribute to the pathogenesis of PD, which has prompted the development of small molecule agents for potential PD therapy, including apedenoson, preladenant,

regadenoson and SYN-115 [24, 58]. Recently, several studies have reported that A2AR antagonism produced far better results in slowing down the pathology and progression of PD and improving symptom management [24, 59–63]. Unfortunately, the majority of these drugs failed in clinical trials except for istradefylline, which has been pursued as a potential PD drug in Phase III clinical trials in Japan [64, 65] but has recently been approved by US Food and Drug Administration as the only non-dopaminergic add-on therapy for the treatment of so-called “off phenomenon” and motor fluctuations of L-dopa therapy in PD [66]. We have suggested that a possible cross-talk between A1Rs and A2ARs could contribute to PD and other neurodegenerative diseases due to elevated adenosine in the ageing brain, which may increase A2AR activation [24, 67–70]. More recently, we reported that chronic stimulation of A1Rs with the A1R agonist CPA led to increased expression of α-Syn both in the SN region of Sprague-Dawley rat brain and in the dopaminergic MN9D cells [25]. Our present *in vitro* findings reported here suggest that drugs that bind to the A1Rs may play a major role in synucleinopathy, independent of their canonical function as A1R agonist or antagonist. We show for the first time that these adenosine-related compounds could bind differentially to different regions of α-Syn, and thus could contribute to α-Syn protein misfolding and the development of α-synucleinopathy in PD. Based on the results from α-Syn domains, we observed that CPA interacted not only with the α-Syn N-terminus but also with α-Syn lacking the NAC region (ΔNAC). However, the A1R antagonist DPCPX significantly altered the population histograms from the nanopore analysis when the N-terminus, C-terminus or the ΔNAC regions were studied, indicating that DPCPX showed binding interactions to all these α-Syn polypeptide domains. Based on the nanopore analysis, we suggest that the two A1R ligands CPA and DPCPX have different binding interactions with α-Syn. Therefore, as we previously suggested for 2-aminoindan [20, 21], CPA could bind to the N-terminus of α-Syn similar to 2-aminoindan thereby leaving the NAC domain free to misfold and cause a higher chance of protein aggregation. In contrast, DPCPX, similar to 1-aminoindan, metformin and caffeine binding to α-Syn, appeared to bind to both the N- and C-termini of α-Syn causing the protein to create a “loop” conformation (Fig. 10) [20, 21]. This loop conformation has been suggested to block the NAC domain from misfolding and hence promote neuroprotection by stopping the misfolded α-Syn protein fibrils from aggregating and forming Lewy Bodies. Therefore, the two possible conformations adopted by α-Syn in the presence of CPA (knot conformation) or DPCPX (loop conformation) (see Fig. 10) are expected to contribute to increased or decreased α-Syn aggregation, respectively.

Additionally, CPA and DPCPX blockade currents possess a remarkable resemblance with those from 2-aminoindan and 1-aminoindan, respectively. The metabolite of Rasagiline, 1-aminoindan, is an irreversible inhibitor of the monoamine oxidase type B enzyme which is administered in mono- and/or poly-therapeutic route to treat early symptoms of PD as well as cognitive impairments and fatigue [71, 72]. Conversely, 2-aminoindan, an amphetamine analogue, is shown to cause PD-like symptoms in long-term users and addicts [73]. Recent case reports indicated that amphetamine and methamphetamine users have a three-fold risk of developing PD compared with nonusers. Interestingly this risk is particularly high in women and it manifests even at 30 years of age [74]. Although 1-aminoindan and 2-

aminoindan have very similar structures they have been shown to hold very different blockade current properties [20, 21].

The blockade histograms for 1-aminoindan demonstrate that most events are related to translocation, as observed previously [20, 21]. In the presence of 10 μM 1-aminoindan, a broad translocation peak at -73 pA and a small bumping peak at -34 pA were observed. It was suggested from nanopore analysis and use of the different α-Syn domains that 1-aminoindan binds to both the N- and C-termini of α-Syn, and by doing so, the drug-protein complex was expected to adopt a “loop” conformation that promotes neuroprotection by preventing α-Syn misfolding. Our present results with both nanopore analysis and molecular dynamics simulations suggest that DPCPX resembled the binding pattern and drug-protein conformation of 1-aminoindan. Conversely, our previous report also established that the 2-aminoindan histograms have two peaks with similar proportion of events, namely the proportion of translocation events is at 48% and bumping events is at 40% [20, 21]. However, 2-aminoindan appeared to bind with higher affinity to α-Syn due to the high binding constant $5*10^4$ M^{-1} derived from isothermal titration calorimetry (ITC), and most importantly because it binds only to the N-terminus of the protein. This N-terminal binding of 2-aminoindan was suggested to promote a neurotoxic “knot” conformation that will lead to increased α-Syn aggregation. We found using nanopore analysis and molecular docking attempts that both adenosine and the selective A1R agonist CPA closely resembled the binding interactions and drug-protein conformations of 2-aminoindan, indicating that these A1R agonists appeared to bind prominently to the N-terminus of α-Syn. Taken together, our results show that CPA and DPCPX, in addition to their canonical function as *bona fide* A1R ligands, also bind to α-Syn to modulate its misfolding and aggregation patterns.

Previous studies using nanopore analysis and a yeast model of PD reported that several compounds that bind to α-Syn, including 1-aminoindan and the dimer compounds containing caffeine linked to 1-aminoindan, nicotine or metformin, can indeed prevent α-Syn aggregation and promote survival in yeast [21, 75, 76]. Moreover, we previously reported that prolonged A1R activation in the brain produced by once daily i.p. injections of rats with CPA (3 mg/kg) for three days led to significant neuronal loss in rat hippocampus *in vivo* [24]. More recently we also reported that longer-term A1R stimulation with 5 mg/kg CPA (i.p. injections daily for 5 weeks) led to increased α-Syn expression and accumulation in the substantia nigral neurons, which was associated with motor and cognitive deficits in Sprague-Dawley rats [25]. Therefore, we tested in the present study whether a shorter duration 7-day chronic injections of either DPCPX or 1-aminoindan could also prevent α-Syn accumulation and aggregation induced by CPA, and whether DPCPX or 1-aminoindan could promote neuroprotection in the substantia nigra of CPA-treated animals. Our results confirmed that 7-day chronic A1R stimulation with CPA upregulated α-Syn expression and increased α-Syn aggregation, which coincided with increased neurodegeneration of dopaminergic neurons in SN *pars compacta*. Suppression of A1R stimulation with DPCPX prevented the neurotoxic effects of CPA. According to our previous report [25], the neurotoxic effect of CPA observed in the present study was likely mediated in part by A1R-induced downstream activation of JNK/cJun and sortilin-dependent binding and accumulation of α-Syn in dopaminergic neurons. Since we found in the

present study that CPA and DPCPX can also bind directly to α-Syn, it would be important to test in future studies using A1R knockout mice or CRISPR/Cas9 gene knockdown of A1Rs in MN9D dopaminergic neurons to determine whether chronic CPA administration can still induce upregulation and accumulation of misfolded α-Syn, and also whether DPCPX or 1-aminoindan can prevent this CPA-induced neurodegeneration of dopaminergic neurons in the absence of functional A1Rs. Since adenosine elevation is widely known to occur in the ageing brain and given the present results indicating that both adenosine and CPA bind to α-Syn N-terminus and cause aggregation, this raises the possibility that increased brain adenosine may be considered a risk factor for increased α-Syn misfolding observed in α-synucleinopathy of PD patients. The results also suggest that targeting α-Syn with adenosine-related compounds (e.g., DPCPX or caffeine) or compounds with similar binding profiles (e.g., 1-aminoindan, metformin, nicotine) may be an attractive therapeutic approach to reduce the neurodegeneration associated with increased accumulation of adenosine in aging-related neurodegenerative diseases.

Conclusion

Nanopore analysis and molecular docking techniques are excellent complimentary tools used to probe potential protein-drug complexes. Importantly, the combination of nanopore analysis and molecular dynamics simulation with our *in vivo* rodent model of α-synucleinopathy in the present study has provided novel insight into the structure and misfolding patterns of the inherently disordered α-Syn protein in the presence of adenosine A1R ligands. Here we demonstrated that adenosine and the A1R agonist CPA bind to the N-terminus of α-Syn, similar to 2-aminoindan, thereby promoting a more compact, neurotoxic knot conformation that leads to increased α-Syn aggregation and neurodegeneration in the substantia nigra. In contrast, the A1R antagonist DPCPX binds to both the N- and C-termini of α-Syn, similar to 1-aminoindan, causing the protein to adopt a neuroprotective loop conformation and thereby reducing neurodegeneration under persistent A1R stimulation. Still, the underlying mechanism of CPA-mediated α-Syn accumulation and aggregation and subsequent neurodegeneration will require further studies. Our recent study demonstrated that chronic A1R stimulation with CPA leads to A1R-dependent accumulation of α-Syn [25], but other plausible explanation for its intracellular accumulation may also involve downstream A1R signaling, reduced vesicular trafficking of α-Syn to the surface membranes, or increased protein stability and reduced degradation of α-Syn upon direct binding with A1R ligands. Therefore, stable inhibition of chronic adenosine A1R stimulation occurring in aged brains of PD patients with clinically approved drugs that also promote a “loop” conformation of α-Syn could be beneficial for possible neuroprotective therapies to decrease α-synucleinopathy in Parkinson’s disease.

Abbreviations

8-Cyclopentyl-1,3-dipropylxanthine – DPCPX; adenosine A1 receptor – A1R; adenosine A2A receptor – A2AR; Alpha-Synuclein – α-Syn; N^6-Cyclopentyladenosine – CPA; Fluoro-Jade C – FJC; Thioflavin S – Thio-S; Tyrosine hydroxylase – TH; Substantia Nigra – SN; Parkinson’s Disease – PD.

Declarations

Ethical Approval and Consent to Participate

Compliance with ethical standards

The authors assert that they have no financial or competing interest. All the biosafety and approvals for the ethical and humane use of animals were obtained prior to the start of the study. All procedures performed in this study were in accordance with the ethical standards of the University of Saskatchewan. The study was approved by the Animal Review and Ethics Board (AREB) of the University of Saskatchewan (Animal Use Protocol # 20070090).

Consent for Publication

All authors have approved the manuscript and consented to publish the data before submitting our paper to the journal.

Availability of data and materials

All the data generated or analyzed during this study are included in this manuscript. Original raw data are available from the University of Saskatchewan (Department of Surgery) and can be readily furnished upon request.

Conflicts of Interests/Competing Interests

The authors have no relevant financial or non-financial interests to disclose.

Funding

This research was funded by the Natural Sciences and Engineering Research Council of Canada Grant (FSC), the Saskatchewan Health Foundation Collaborative Innovation and Development Grant (FSC and JSL), the Heart and Stroke Foundation of Canada (FSC), and Canada Foundation for Innovation Leaders Opportunity Fund (FSC).

Authors' contributions

E.J. performed and analyzed the nanopore assay and histological/confocal imaging microscopy analysis. M.T.M. carried out the structural modeling analysis. E.J. and F.S.C. wrote the manuscript; M.T.M., J.S.L. and M.B. helped in revising the manuscript. All authors read and approved the final manuscript.

Acknowledgments

F.S.C. received funding support from Heart and Stroke Foundation of Canada, NSERC Discovery Grant, Saskatchewan Health Research Foundation (SHRF), and College of Medicine (University of

Saskatchewan). J.S.L. was supported by NSERC Discovery Grant. M.B. received support from NSERC Discovery Grant, Canadian Institutes of Health Research (CIHR), and SHRF. E.J. received Doctoral Award from College of Medicine, University of Saskatchewan. M.T.M. received SHRF Postdoctoral Fellowship.

References

1. Gillis, P, and J S Malter. 1991. The adenosine-uridine binding factor recognizes the AU-rich elements of cytokine, lymphokine, and oncogene mRNAs. *Journal of Biological Chemistry* 266: 3172–3177.
2. Bours, M J L, E L R Swennen, F Di Virgilio, B N Cronstein, and P C Dagnelie. 2006. Adenosine 5'-triphosphate and adenosine as endogenous signaling molecules in immunity and inflammation. *Pharmacology & Therapeutics* 112: 358–404. doi:https://doi.org/10.1016/j.pharmthera.2005.04.013.
3. Touyz, Rhian M, and Ana M Briones. 2010. Reactive oxygen species and vascular biology: implications in human hypertension. *Hypertension Research* 34. The Japanese Society of Hypertension: 5.
4. Burnstock, G, and A Verkhratsky. 2010. Long-term (trophic) purinergic signalling: purinoceptors control cell proliferation, differentiation and death. *Cell Death &Amp; Disease* 1. The Author(s): e9.
5. Cao, Xiong, Liang-Ping Li, Xi-He Qin, Shu-Ji Li, Meng Zhang, Qian Wang, Hong-Hai Hu, et al. 2013. Astrocytic Adenosine 5'-Triphosphate Release Regulates the Proliferation of Neural Stem Cells in the Adult Hippocampus. *STEM CELLS* 31. John Wiley & Sons, Ltd: 1633–1643. doi:10.1002/stem.1408.
6. Abbracchio, Maria P, Geoffrey Burnstock, Alexei Verkhratsky, and Herbert Zimmermann. 2009. Purinergic signalling in the nervous system: an overview. *Trends in Neurosciences* 32: 19–29. doi:https://doi.org/10.1016/j.tins.2008.10.001.
7. Eltzschig, Holger K, and Tobias Eckle. 2011. Ischemia and reperfusion—from mechanism to translation. *Nature Medicine* 17. Nature Publishing Group, a division of Macmillan Publishers Limited. All Rights Reserved.: 1391.
8. Pagonopoulou, O, A Efthimiadou, B Asimakopoulos, and N K Nikolettos. 2006. Modulatory role of adenosine and its receptors in epilepsy: Possible therapeutic approaches. *Neuroscience Research* 56: 14–20. doi:https://doi.org/10.1016/j.neures.2006.05.010.
9. Frenguelli, Nicholas Dale and Bruno G. 2009. Release of Adenosine and ATP During Ischemia and Epilepsy. *Current Neuropharmacology*. doi:http://dx.doi.org/10.2174/157015909789152146.
10. Ferré, Sergi, Francisco Ciruela, Meritxell Canals, Daniel Marcellino, Javier Burgueno, Vicent Casadó, Joëlle Hillion, et al. 2004. Adenosine A2A-dopamine D2 receptor–receptor heteromers. Targets for neuro-psychiatric disorders. *Parkinsonism & Related Disorders* 10: 265–271. doi:https://doi.org/10.1016/j.parkreldis.2004.02.014.
11. Saitoh, Masaru, Kaoru Nagai, Kazuhiko Nakagawa, Takehira Yamamura, Satoshi Yamamoto, and Tomoyuki Nishizaki. 2004. Adenosine induces apoptosis in the human gastric cancer cells via an

intrinsic pathway relevant to activation of AMP-activated protein kinase. *Biochemical Pharmacology* 67: 2005–2011. doi:https://doi.org/10.1016/j.bcp.2004.01.020.

12. Manwani, Bharti, and Louise D McCullough. 2013. Function of the master energy regulator adenosine monophosphate-activated protein kinase in stroke. *Journal of Neuroscience Research* 91. John Wiley & Sons, Ltd: 1018–1029. doi:10.1002/jnr.23207.
13. Angulo, Ester, Vicent Casadó, Josefa Mallol, Enric I Canela, Francesc Viñals, Isidre Ferrer, Carmen Lluis, and Rafael Franco. 2006. A1 Adenosine Receptors Accumulate in Neurodegenerative Structures in Alzheimer's Disease and Mediate Both Amyloid Precursor Protein Processing and Tau Phosphorylation and Translocation. *Brain Pathology* 13. John Wiley & Sons, Ltd: 440–451. doi:10.1111/j.1750-3639.2003.tb00475.x.
14. Jansen, K L R, R L M Faull, M Dragunow, and B L Synek. 1990. Alzheimer's disease: Changes in hippocampal N-methyl-d-aspartate, quisqualate, neurotensin, adenosine, benzodiazepine, serotonin and opioid receptors—an autoradiographic study. *Neuroscience* 39: 613–627. doi:https://doi.org/10.1016/0306-4522(90)90246-Z.
15. Morelli, Micaela, Anna R Carta, and Peter Jenner. 2009. Adenosine A2A Receptors and Parkinson's Disease. In *Adenosine Receptors in Health and Disease*, ed. Constance N. Wilson and S. Jamal Mustafa, 589–615. Berlin, Heidelberg: Springer Berlin Heidelberg. doi:10.1007/978-3-540-89615-9_18.
16. de Lau, Lonneke M L, and Monique M B Breteler. 2006. Epidemiology of Parkinson's disease. *The Lancet Neurology* 5: 525–535. doi:https://doi.org/10.1016/S1474-4422(06)70471-9.
17. Ingelsson, Martin. 2016. Alpha-Synuclein Oligomers—Neurotoxic Molecules in Parkinson's Disease and Other Lewy Body Disorders . *Frontiers in Neuroscience* .
18. Dauer, William, and Serge Przedborski. 2003. Parkinson's Disease: Mechanisms and Models. *Neuron* 39: 889–909. doi:https://doi.org/10.1016/S0896-6273(03)00568-3.
19. Spillantini, Maria Grazia, R Anthony Crowther, Ross Jakes, Masato Hasegawa, and Michel Goedert. 1998. α-Synuclein in filamentous inclusions of Lewy bodies from Parkinson's disease and dementia with Lewy bodies. *Proceedings of the National Academy of Sciences* 95: 6469 LP – 6473.
20. Kakish, Joe, Dongsoo Lee, and Jeremy S Lee. 2015. Drugs That Bind to α-Synuclein: Neuroprotective or Neurotoxic? *ACS Chemical Neuroscience* 6. American Chemical Society: 1930–1940. doi:10.1021/acschemneuro.5b00172.
21. Jakova, E., and J.S. Lee. 2017. Behavior of α-synuclein–drug complexes during nanopore analysis with a superimposed AC field. *Electrophoresis* 38. doi:10.1002/elps.201600253.
22. Tripathi, Richa, Hamidreza Saber, Varun Chauhan, Kaushalendra Tripathi, and Stewart Factor. 2018. Parkinson Disease from long term drug abuse: Meta-analysis of amphetamine/methamphetamine and Parkinson Disease (P6.079). *Neurology* 90: P6.079.
23. Pregeljc, Domen, Diana Teodorescu-Perijoc, Robert Vianello, Nejc Umek, and Janez Mavri. 2019. How Important Is the Use of Cocaine and Amphetamines in the Development of Parkinson Disease? A Computational Study. *Neurotoxicity Research*. doi:10.1007/s12640-019-00149-0.

24. Stockwell, J., E. Jakova, and F.S. Cayabyab. 2017. Adenosine A1 and A2A receptors in the brain: Current research and their role in neurodegeneration. *Molecules* 22. doi:10.3390/molecules22040676.
25. Lv, Yun-Cheng, An-Bo Gao, Jing Yang, Li-Yuan Zhong, Bo Jia, Shu-Hui Ouyang, Le Gui, Tian-Hong Peng, Sha Sun, and Francisco S Cayabyab. 2020. Long-term adenosine A1 receptor activation-induced sortilin expression promotes α-synuclein upregulation in dopaminergic neurons. *Neural regeneration research* 15. Medknow Publications: 712.
26. Shen, Ke-Zhong, and Steven W Johnson. 1997. Presynaptic GABAB and adenosine A1 receptors regulate synaptic transmission to rat substantia nigra reticulata neurones. *The Journal of Physiology* 505. John Wiley & Sons, Ltd: 153–163. doi:10.1111/j.1469-7793.1997.153bc.x.
27. Liu, Da-Zhi, Ke-Qiang Xie, Xin-Quan Ji, Yang Ye, Cheng-Liang Jiang, and Xing-Zu Zhu. 2005. Neuroprotective effect of paeoniflorin on cerebral ischemic rat by activating adenosine A1 receptor in a manner different from its classical agonists. *British Journal of Pharmacology* 146. John Wiley & Sons, Ltd: 604–611. doi:10.1038/sj.bjp.0706335.
28. Wang, Yi-Ting, Hui-Ching Lin, Wei-Zhong Zhao, Hui-Ju Huang, Yu-Li Lo, Hsiang-Tsui Wang, and Anya Maan-Yuh Lin. 2017. Acrolein acts as a neurotoxin in the nigrostriatal dopaminergic system of rat: involvement of α-synuclein aggregation and programmed cell death. *Scientific Reports* 7: 45741. doi:10.1038/srep45741.
29. Tapias, Victor, Xiaoping Hu, Kelvin C Luk, Laurie H Sanders, Virginia M Lee, and J Timothy Greenamyre. 2017. Synthetic alpha-synuclein fibrils cause mitochondrial impairment and selective dopamine neurodegeneration in part via iNOS-mediated nitric oxide production. *Cellular and Molecular Life Sciences* 74: 2851–2874. doi:10.1007/s00018-017-2541-x.
30. Hu, Qidi, Xiangpeng Ren, Ya Liu, Zhihui Li, Liping Zhang, Xingjun Chen, Chaoxiang He, and Jiang-Fan Chen. 2016. Aberrant adenosine A2A receptor signaling contributes to neurodegeneration and cognitive impairments in a mouse model of synucleinopathy. *Experimental Neurology* 283: 213–223. doi:https://doi.org/10.1016/j.expneurol.2016.05.040.
31. Schmued, Larry C, Chris C Stowers, Andrew C Scallet, and Lulu Xu. 2005. Fluoro-Jade C results in ultra high resolution and contrast labeling of degenerating neurons. *Brain Research* 1035: 24–31. doi:https://doi.org/10.1016/j.brainres.2004.11.054.
32. Lee, He-Jin, Soon Young Shin, Chan Choi, Young Han Lee, and Seung-Jae Lee. 2002. Formation and Removal of α-Synuclein Aggregates in Cells Exposed to Mitochondrial Inhibitors. *Journal of Biological Chemistry* 277: 5411–5417. doi:10.1074/jbc.M105326200.
33. Madampage, Claudia A, Omid Tavassoly, Chris Christensen, Meena Kumari, and Jeremy S Lee. 2012. Nanopore analysis. *Prion* 6. Taylor & Francis: 116–123. doi:10.4161/pri.18665.
34. Jakova, Elisabet, and Jeremy S. Lee. 2015. Superposition of an AC field improves the discrimination between peptides in nanopore analysis. *Analyst* 140: 4813–4819. doi:10.1039/c4an02180k.
35. Christensen, Christopher, Christian Baran, Besnik Krasniqi, Radu I Stefureac, Sergiy Nokhrin, and Jeremy S Lee. 2011. Effect of charge, topology and orientation of the electric field on the interaction

of peptides with the α-hemolysin pore. *Journal of Peptide Science* 17. John Wiley & Sons, Ltd: 726–734. doi:10.1002/psc.1393.

36. Meng, Howard, Dielle Detillieux, Christian Baran, Besnik Krasniqi, Christopher Christensen, Claudia Madampage, Radu I Stefureac, and Jeremy S Lee. 2010. Nanopore analysis of tethered peptides. *Journal of Peptide Science* 16. John Wiley & Sons, Ltd: 701–708. doi:10.1002/psc.1289.
37. Malty, Ramy H, Matthew Jessulat, Ke Jin, Gabriel Musso, James Vlasblom, Sadhna Phanse, Zhaolei Zhang, and Mohan Babu. 2015. Mitochondrial Targets for Pharmacological Intervention in Human Disease. *Journal of Proteome Research* 14. American Chemical Society: 5–21. doi:10.1021/pr500813f.
38. Moutaoufik, Mohamed Taha, Ramy Malty, Shahreen Amin, Qingzhou Zhang, Sadhna Phanse, Alla Gagarinova, Mara Zilocchi, et al. 2019. Rewiring of the Human Mitochondrial Interactome during Neuronal Reprogramming Reveals Regulators of the Respirasome and Neurogenesis. *iScience* 19: 1114–1132. doi:https://doi.org/10.1016/j.isci.2019.08.057.
39. Rotem, Dvir, Lakmal Jayasinghe, Maria Salichou, and Hagan Bayley. 2012. Protein Detection by Nanopores Equipped with Aptamers. *Journal of the American Chemical Society* 134. American Chemical Society: 2781–2787. doi:10.1021/ja2105653.
40. Venkatesan, Bala Murali, and Rashid Bashir. 2011. Nanopore sensors for nucleic acid analysis. *Nature Nanotechnology* 6. Nature Publishing Group, a division of Macmillan Publishers Limited. All Rights Reserved.: 615.
41. Yang, Jianyi, Ivan Anishchenko, Hahnbeom Park, Zhenling Peng, Sergey Ovchinnikov, and David Baker. 2020. Improved protein structure prediction using predicted interresidue orientations. *Proceedings of the National Academy of Sciences* 117: 1496 LP – 1503. doi:10.1073/pnas.1914677117.
42. Ulmer, Tobias S, Ad Bax, Nelson B Cole, and Robert L Nussbaum. 2005. Structure and dynamics of micelle-bound human α-synuclein. *Journal of Biological Chemistry* 280. ASBMB: 9595–9603.
43. Chen, Zhicheng, Cherry Xiong, Cassandra Pancyr, Jocelyn Stockwell, Wolfgang Walz, and Francisco S Cayabyab. 2014. Prolonged Adenosine A1 Receptor Activation in Hypoxia and Pial Vessel Disruption Focal Cortical Ischemia Facilitates Clathrin-Mediated AMPA Receptor Endocytosis and Long-Lasting Synaptic Inhibition in Rat Hippocampal CA3-CA1 Synapses: Differential Regulat. *The Journal of Neuroscience* 34: 9621 LP – 9643. doi:10.1523/JNEUROSCI.3991-13.2014.
44. Fredholm, Bertil B, Karl Bättig, Janet Holmén, Astrid Nehlig, and Edwin E Zvartau. 1999. Actions of Caffeine in the Brain with Special Reference to Factors That Contribute to Its Widespread Use. *Pharmacological Reviews* 51: 83 LP – 133.
45. Daly, John W, Pamela Butts-Lamb, and William Padgett. 1983. Subclasses of adenosine receptors in the central nervous system: Interaction with caffeine and related methylxanthines. *Cellular and Molecular Neurobiology* 3: 69–80. doi:10.1007/BF00734999.
46. Biaggioni, I, S Paul, A Puckett, and C Arzubiaga. 1991. Caffeine and theophylline as adenosine receptor antagonists in humans. *Journal of Pharmacology and Experimental Therapeutics* 258: 588

LP – 593.

47. Tavassoly, Omid, Joe Kakish, Sergiy Nokhrin, Oleg Dmitriev, and Jeremy S Lee. 2014. The use of nanopore analysis for discovering drugs which bind to α-synuclein for treatment of Parkinson's disease. *European Journal of Medicinal Chemistry* 88: 42–54. doi:https://doi.org/10.1016/j.ejmech.2014.07.090.
48. Breckenridge, Charles B, Nicholas C Sturgess, Mark Butt, Jeffrey C Wolf, Dan Zadory, Melissa Beck, James M Mathews, et al. 2013. Pharmacokinetic, neurochemical, stereological and neuropathological studies on the potential effects of paraquat in the substantia nigra pars compacta and striatum of male C57BL/6J mice. *NeuroToxicology* 37: 1–14. doi:https://doi.org/10.1016/j.neuro.2013.03.005.
49. Takahashi, H, Y Watanabe, H Tanaka, M Mihara, H Mochizuki, K Takahashi, K Yamamoto, T Liu, Y Wang, and N Tomiyama. 2018. Comprehensive MRI quantification of the substantia nigra pars compacta in Parkinson's disease. *European Journal of Radiology* 109: 48–56. doi:https://doi.org/10.1016/j.ejrad.2018.06.024.
50. Surmeier, Dalton James. 2018. Determinants of dopaminergic neuron loss in Parkinson's disease. *The FEBS Journal* 285. John Wiley & Sons, Ltd: 3657–3668. doi:10.1111/febs.14607.
51. Tomlinson, Claire L, Rebecca Stowe, Smitaa Patel, Caroline Rick, Richard Gray, and Carl E Clarke. 2010. Systematic review of levodopa dose equivalency reporting in Parkinson's disease. *Movement disorders* 25. Wiley Online Library: 2649–2653.
52. Marsden, C D, and J D Parkes. 1977. SUCCESS AND PROBLEMS OF LONG-TERM LEVODOPA THERAPY IN PARKINSON'S DISEASE. *The Lancet* 309: 345–349. doi:https://doi.org/10.1016/S0140-6736(77)91146-1.
53. Olanow, C Warren, Jose A Obeso, and Fabrizio Stocchi. 2006. Continuous dopamine-receptor treatment of Parkinson's disease: scientific rationale and clinical implications. *The Lancet Neurology* 5: 677–687. doi:https://doi.org/10.1016/S1474-4422(06)70521-X.
54. Bonifácio, Maria João, P Nuno Palma, Luís Almeida, and Patrício Soares-da-Silva. 2007. Catechol-O-methyltransferase and Its Inhibitors in Parkinson's Disease. *CNS Drug Reviews* 13. John Wiley & Sons, Ltd (10.1111): 352–379. doi:10.1111/j.1527-3458.2007.00020.x.
55. Group, Parkinson Study. 2005. A randomized placebo-controlled trial of rasagiline in levodopa-treated patients with parkinson disease and motor fluctuations: The presto study. *Archives of Neurology* 62: 241–248.
56. Horstink, M, E Tolosa, U Bonuccelli, G Deuschl, A Friedman, P Kanovsky, J P Larsen, et al. 2006. Review of the therapeutic management of Parkinson's disease. Report of a joint task force of the European Federation of Neurological Societies and the Movement Disorder Society–European Section. Part I: early (uncomplicated) Parkinson's disease. *European Journal of Neurology* 13. John Wiley & Sons, Ltd (10.1111): 1170–1185. doi:10.1111/j.1468-1331.2006.01547.x.
57. Schade, René, Frank Andersohn, Samy Suissa, Wilhelm Haverkamp, and Edeltraut Garbe. 2007. Dopamine Agonists and the Risk of Cardiac-Valve Regurgitation. *New England Journal of Medicine*

356. Massachusetts Medical Society: 29–38. doi:10.1056/NEJMoa062222.

58. Ferreira, Diana G, Vânia L Batalha, Hugo Vicente Miranda, Joana E Coelho, Rui Gomes, Francisco Q Gonçalves, Joana I Real, et al. 2017. Adenosine A2A Receptors Modulate α-Synuclein Aggregation and Toxicity. *Cerebral cortex (New York, N.Y.: 1991)* 27: 718—730. doi:10.1093/cercor/bhv268.
59. Schwarzschild, Michael A, Luigi Agnati, Kjell Fuxe, Jiang-Fan Chen, and Micaela Morelli. 2006. Targeting adenosine A2A receptors in Parkinson's disease. *Trends in Neurosciences* 29: 647–654. doi:https://doi.org/10.1016/j.tins.2006.09.004.
60. Factor, Stewart A, Kenneth Wolski, Daniel M Togasaki, Susan Huyck, Marc Cantillon, T W Ho, Robert A Hauser, and Emmanuelle Pourcher. 2013. Long-term safety and efficacy of preladenant in subjects with fluctuating Parkinson's disease. *Movement Disorders* 28. John Wiley & Sons, Ltd: 817–820. doi:10.1002/mds.25395.
61. Mizuno, Yoshikuni, Kazuko Hasegawa, Tomoyoshi Kondo, Sadako Kuno, and Mitsutoshi Yamamoto. 2010. Clinical efficacy of istradefylline (KW-6002) in Parkinson's disease: A randomized, controlled study. *Movement Disorders* 25. John Wiley & Sons, Ltd: 1437–1443. doi:10.1002/mds.23107.
62. Prediger, Rui D S. 2010. Effects of caffeine in Parkinson's disease: from neuroprotection to the management of motor and non-motor symptoms. *Journal of Alzheimer's Disease* 20. IOS Press: S205–S220.
63. Postuma, Ronald B, Anthony E Lang, Renato P Munhoz, Katia Charland, Amelie Pelletier, Mariana Moscovich, Luciane Filla, et al. 2012. Caffeine for treatment of Parkinson disease. *Neurology* 79: 651 LP – 658. doi:10.1212/WNL.0b013e318263570d.
64. Kondo, Tomoyoshi, Yoshikuni Mizuno, and Japanese Istradefylline Study Group. 2015. A Long-Term Study of Istradefylline Safety and Efficacy in Patients With Parkinson Disease. *Clinical Neuropharmacology* 38.
65. Vorovenci, Ruxandra Julia, and Angelo Antonini. 2015. The efficacy of oral adenosine A2A antagonist istradefylline for the treatment of moderate to severe Parkinson's disease. *Expert Review of Neurotherapeutics* 15. Taylor & Francis: 1383–1390. doi:10.1586/14737175.2015.1113131.
66. Chen, Jiang-Fan, and Rodrigo A Cunha. 2020. The belated US FDA approval of the adenosine A 2A receptor antagonist istradefylline for treatment of Parkinson's disease. *Purinergic Signalling*. Springer: 1–8.
67. Stockwell, Jocelyn, Zhicheng Chen, Mina Niazi, Siddarth Nosib, and Francisco S Cayabyab. 2016. Protein phosphatase role in adenosine A1 receptor-induced AMPA receptor trafficking and rat hippocampal neuronal damage in hypoxia/reperfusion injury. *Neuropharmacology* 102: 254–265. doi:https://doi.org/10.1016/j.neuropharm.2015.11.018.
68. Chen, Zhicheng, Jocelyn Stockwell, and Francisco S Cayabyab. 2016. Adenosine A1 Receptor-Mediated Endocytosis of AMPA Receptors Contributes to Impairments in Long-Term Potentiation (LTP) in the Middle-Aged Rat Hippocampus. *Neurochemical Research* 41: 1085–1097. doi:10.1007/s11064-015-1799-3.

69. Chen, Zhicheng, Cherry Xiong, Cassandra Pancyr, Jocelyn Stockwell, Wolfgang Walz, and Francisco S Cayabyab. 2014. Prolonged Adenosine A1 Receptor Activation in Hypoxia and Pial Vessel Disruption Focal Cortical Ischemia Facilitates Clathrin-Mediated AMPA Receptor Endocytosis and Long-Lasting Synaptic Inhibition in Rat Hippocampal CA3-CA1 Synapses: Differential Regulat. *The Journal of Neuroscience* 34: 9621 LP – 9643.
70. Qin, X., Zaki, M.G., Chen, Z., Jakova, E., Ming, Z., and Cayabyab, F.S. 2020. Adenosine Signaling and Clathrin-mediated Endocytosis of Glutamate AMPA Receptors in Delayed Hypoxic Injury in Rat Hippocampus: Role of Casein Kinase 2. *Molecular neurobiology*.
71. Olanow, C Warren, Olivier Rascol, Robert Hauser, Paul D Feigin, Joseph Jankovic, Anthony Lang, William Langston, et al. 2009. A Double-Blind, Delayed-Start Trial of Rasagiline in Parkinson's Disease. *New England Journal of Medicine* 361. Massachusetts Medical Society: 1268–1278. doi:10.1056/NEJMoa0809335.
72. Group, Parkinson Study. 2004. A controlled, randomized, delayed-start study of rasagiline in early parkinson disease. *Archives of Neurology* 61: 561–566.
73. Callaghan, Russell C, James K Cunningham, Jenna Sykes, and Stephen J Kish. 2012. Increased risk of Parkinson's disease in individuals hospitalized with conditions related to the use of methamphetamine or other amphetamine-type drugs. *Drug and Alcohol Dependence* 120: 35–40. doi:https://doi.org/10.1016/j.drugalcdep.2011.06.013.
74. Curtin, Karen, Annette E Fleckenstein, Reid J Robison, Michael J Crookston, Ken R Smith, and Glen R Hanson. 2015. Methamphetamine/amphetamine abuse and risk of Parkinson's disease in Utah: A population-based assessment. *Drug and Alcohol Dependence* 146: 30–38. doi:https://doi.org/10.1016/j.drugalcdep.2014.10.027.
75. Kakish, Joe, Omid Tavassoly, and Jeremy S Lee. 2014. Rasagiline, a suicide inhibitor of monoamine oxidases, binds reversibly to α-synuclein. *ACS chemical neuroscience* 6. ACS Publications: 347–355.
76. Kakish, Joe, Kevin J H Allen, Troy A Harkness, Ed S Krol, and Jeremy S Lee. 2016. Novel Dimer Compounds That Bind α-Synuclein Can Rescue Cell Growth in a Yeast Model Overexpressing α-Synuclein. A Possible Prevention Strategy for Parkinson's Disease. *ACS Chemical Neuroscience* 7. American Chemical Society: 1671–1680. doi:10.1021/acschemneuro.6b00209.

Figures

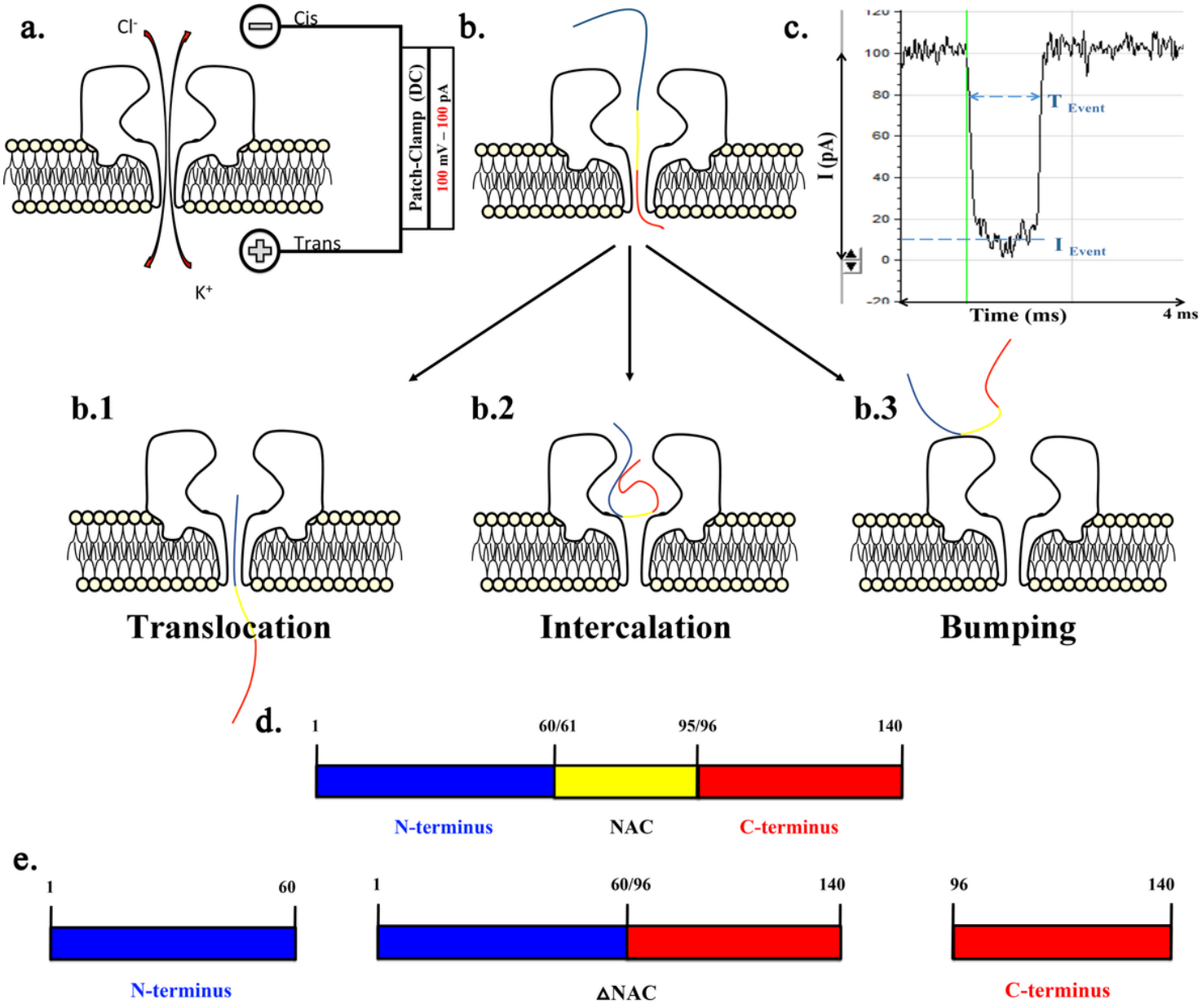

Figure 1

Nanopore analysis setup and α-Synuclein interaction with the α-Hemolysin pore. a. The patch-clamp setup at 100 mV direct current (DC) allows the ions to flow in the pore and create an ionic current b. The interruption of the current when α-Synuclein interacts with the pore forming three distinguishable blockade current events: b.1 Translocation events, where α-Synuclein goes through the pore causing a large current blockade (as seen in Figure 1 c); b.2 Intercalation events, where α-Synuclein is trapped in the pore entrance, but will diffuse back after a period of time causing an intermediate current blockade; and b.3 Bumping events, where α-Synuclein approaches the pore, but diffuses away without entering causing a small current blockade. c. The disruption of the blockade current and time caused by α-Synuclein when the protein translocates the pore. d. α-Synuclein full sequence and e. The domains of α-Synuclein used in the nanopore setup consisting of: N-terminus (blue); ΔNAC, the entire sequence of α-Synuclein without the non-Amyloidβ-component region (blue and red); and C-terminus (red).

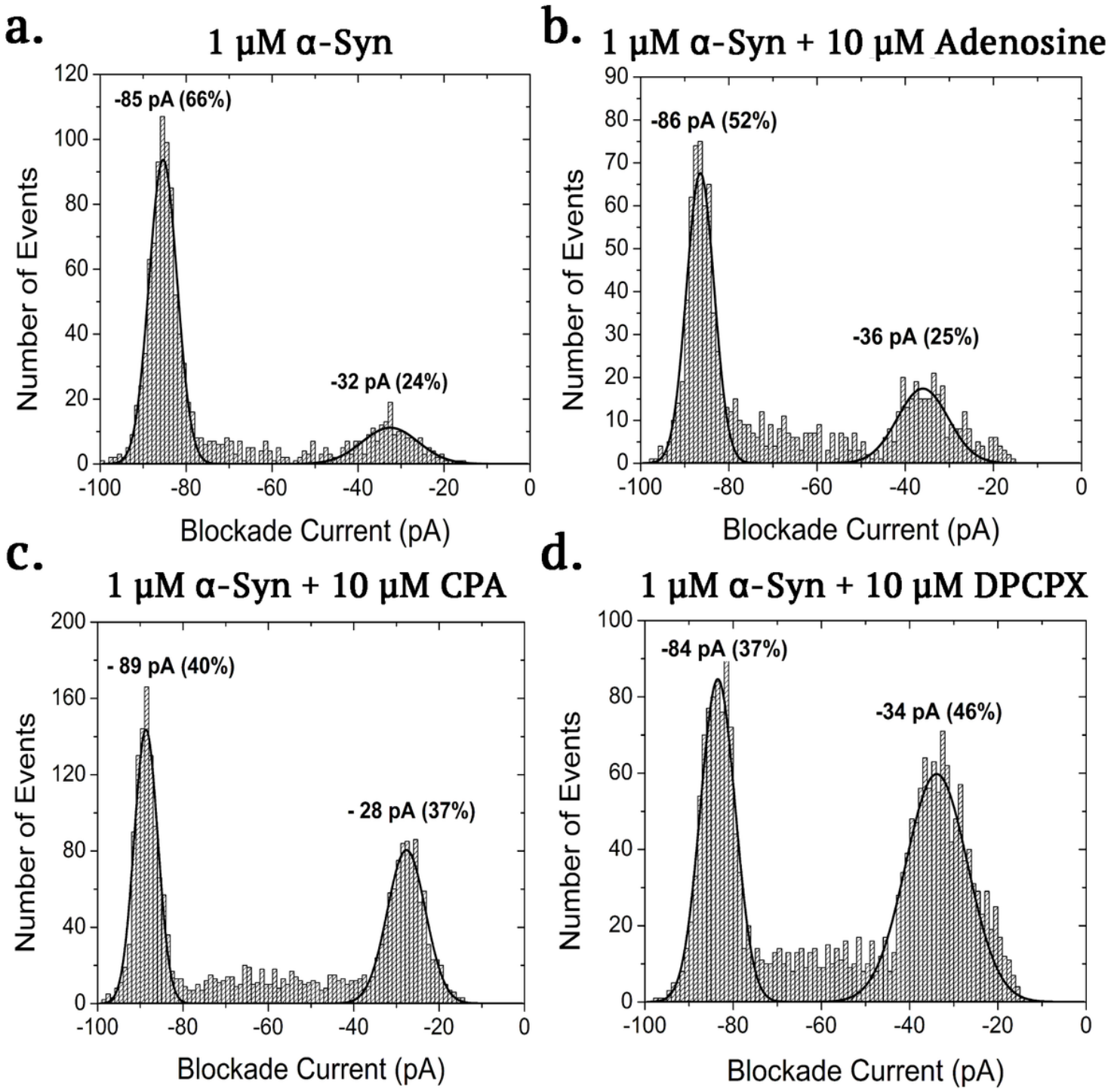

Figure 2

Representative blockade current histograms of a. 1 µM α-Synuclein alone and with b. 10 µM Adenosine, c. 10 µM CPA and d. 10 µM DPCPX at 100 mV DC indicating binding to the protein Each experiment was run in triplicates and the standard error of the mean estimated for the percentage of events is <±10% (see Table 1).

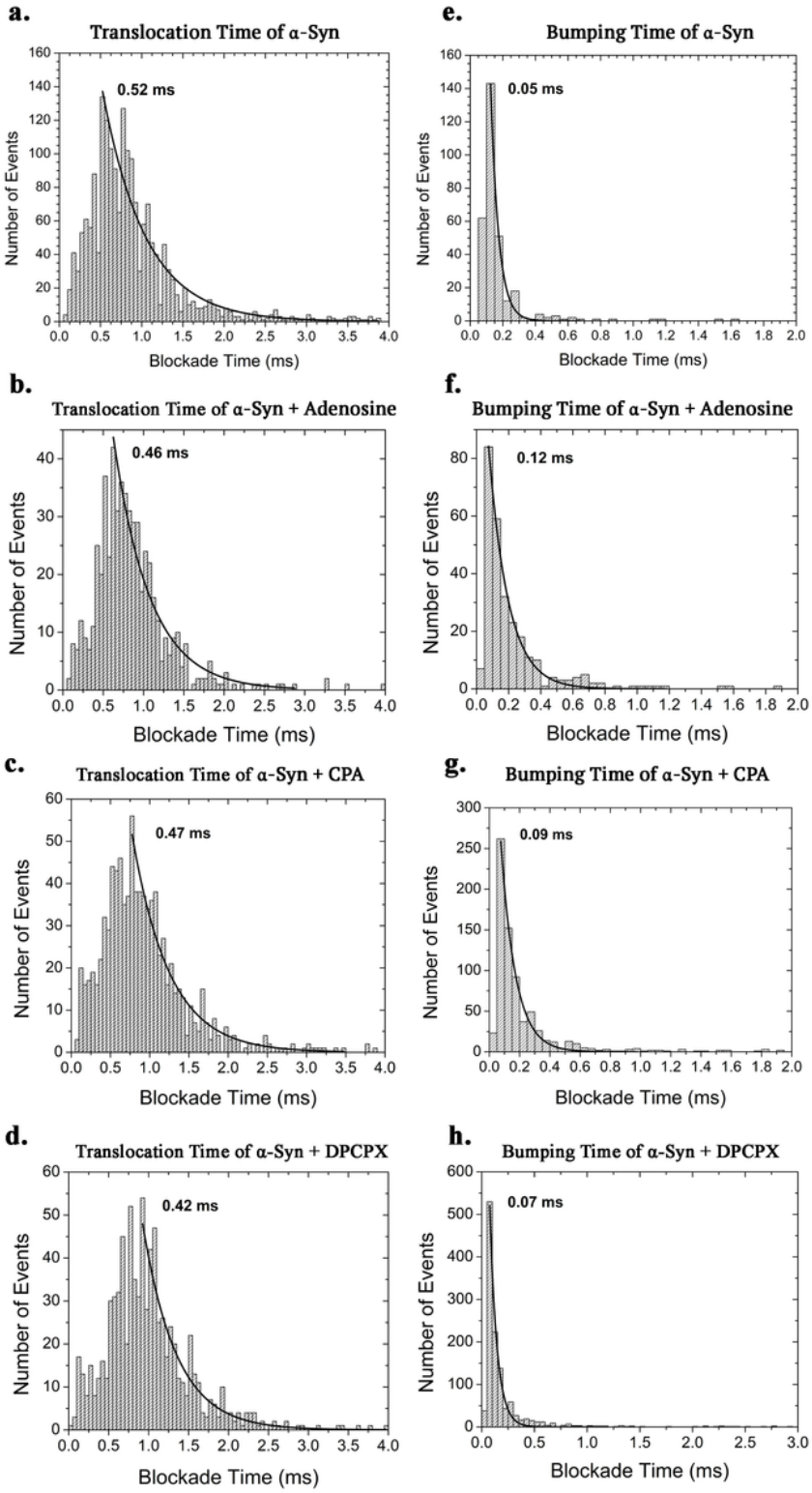

Figure 3

Representative blockade time profiles of translocation events (panels a.-d.) and bumping events (panels e.-f.) for 1 μM α-Synuclein alone and in the presence of 10 μM Adenosine, 10 μM CPA and 10 μM DPCPX. (Each experiment was run in triplicates). For mean and SEM values of populations of translocation and bumping and blockade times in absence or presence of adenosine, CPA or DPCPX, please see Table 1.

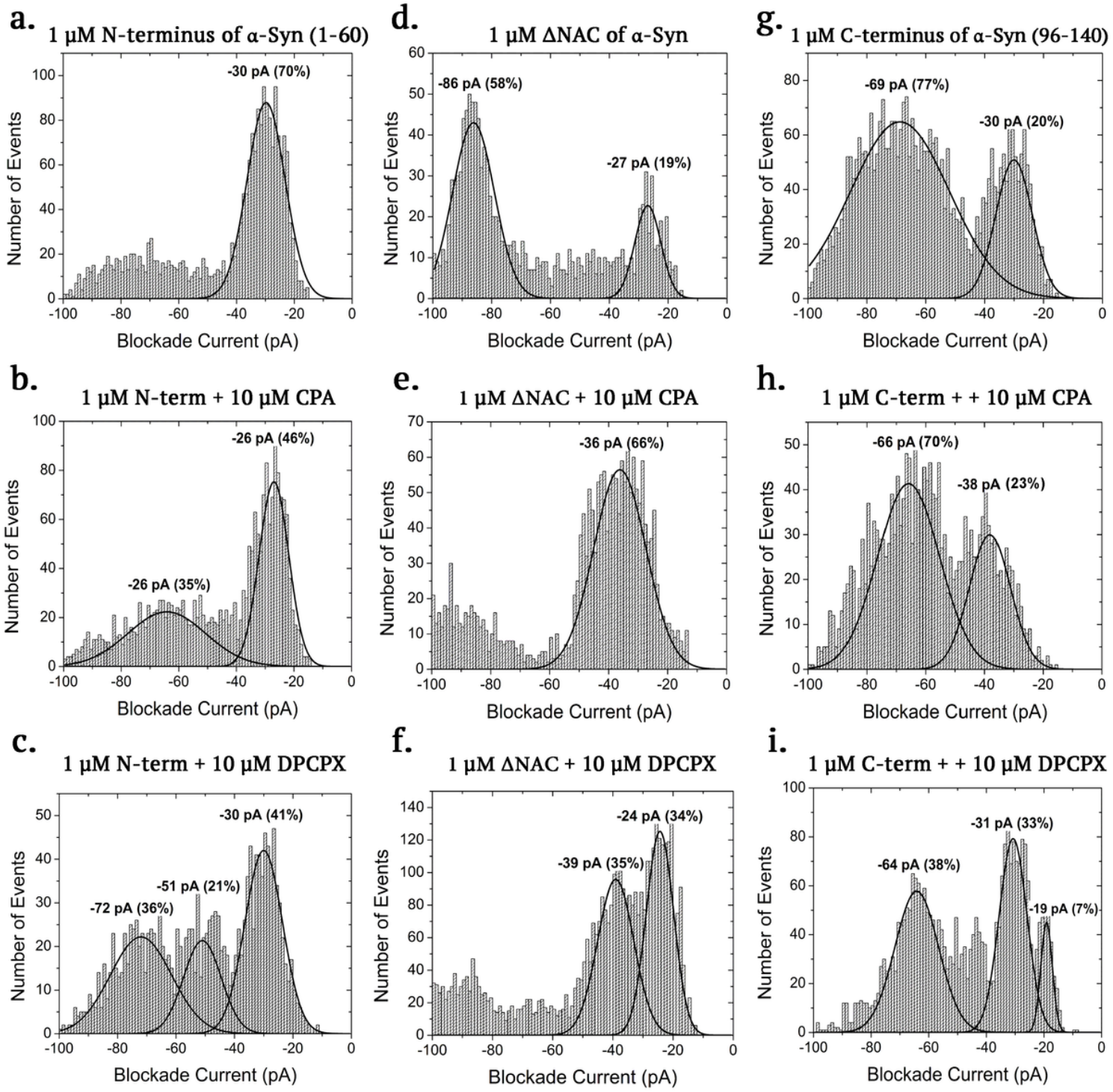

Figure 4

Representative blockade current histograms of 10 µM CPA and 10 µM DPCPX with N-terminus (a.-c.), ΔNAC (d.-f.) and C-terminus (g.-i.) of α-Synuclein at 100 mV DC. Each experiment was run in triplicates and the error estimated for the percentage of events is <±10% (see Table 2).

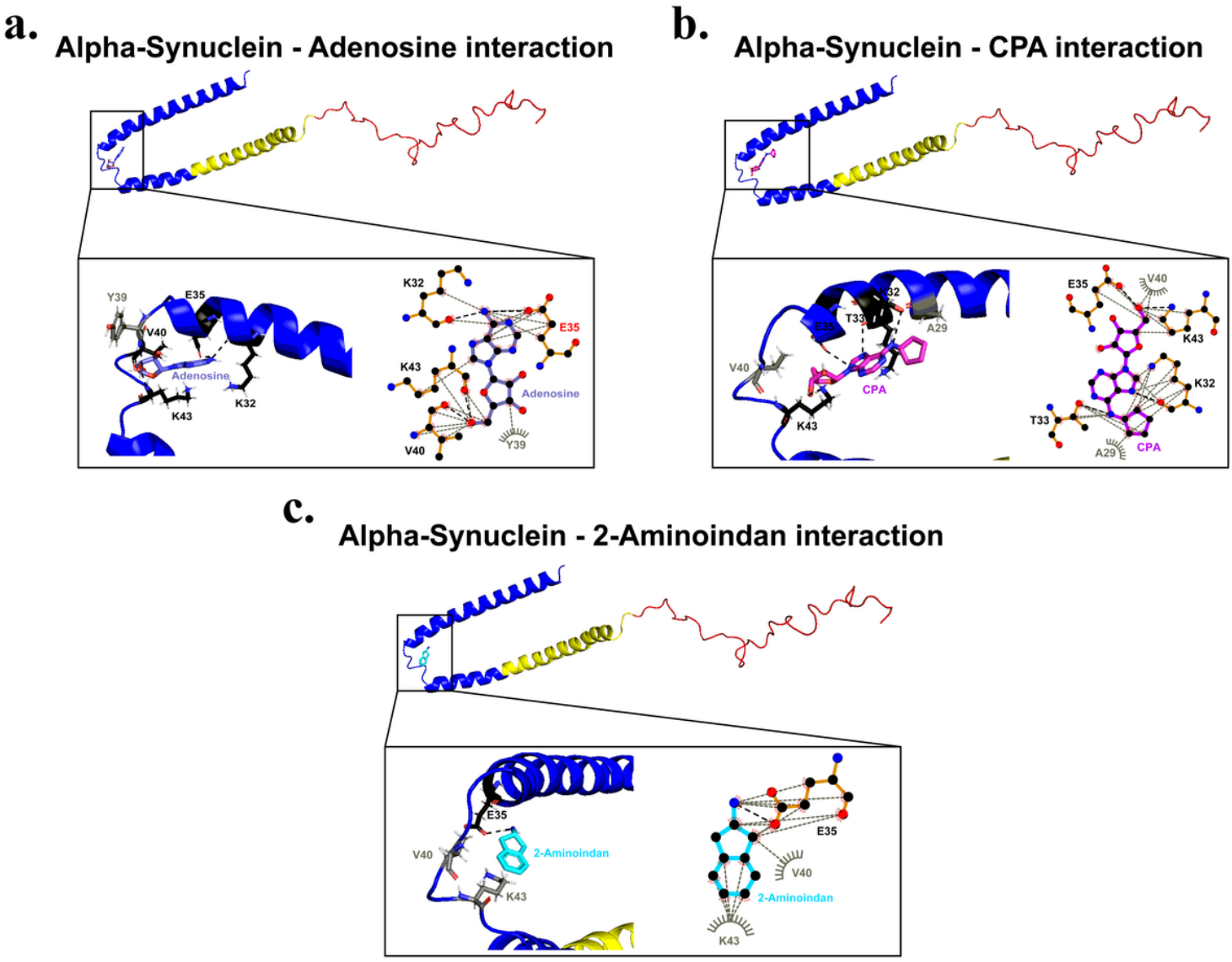

Figure 5

Molecular docking simulation of 1XQ8 α-Synuclein structure bound to adenosine, CPA and 2-aminoindan. In each group the first image is the full 3D representation of the docking of α-Synuclein (blue is the N-terminus, yellow the NAC component and red the C-terminus) bound to a. adenosine, b. CPA, and c. 2-aminoindan. Below the full 3D representations are shown with the magnified binding pocket of α-Synuclein and the amino acid residue locations responsible for each drug binding. Black dashed lines indicate hydrogen bonding. The molecular docking study was carried out using Autodock Vina module implemented in PyRx tool. Protein and ligand interactions were analyzed and visualized through Pymol and LigPlot+.

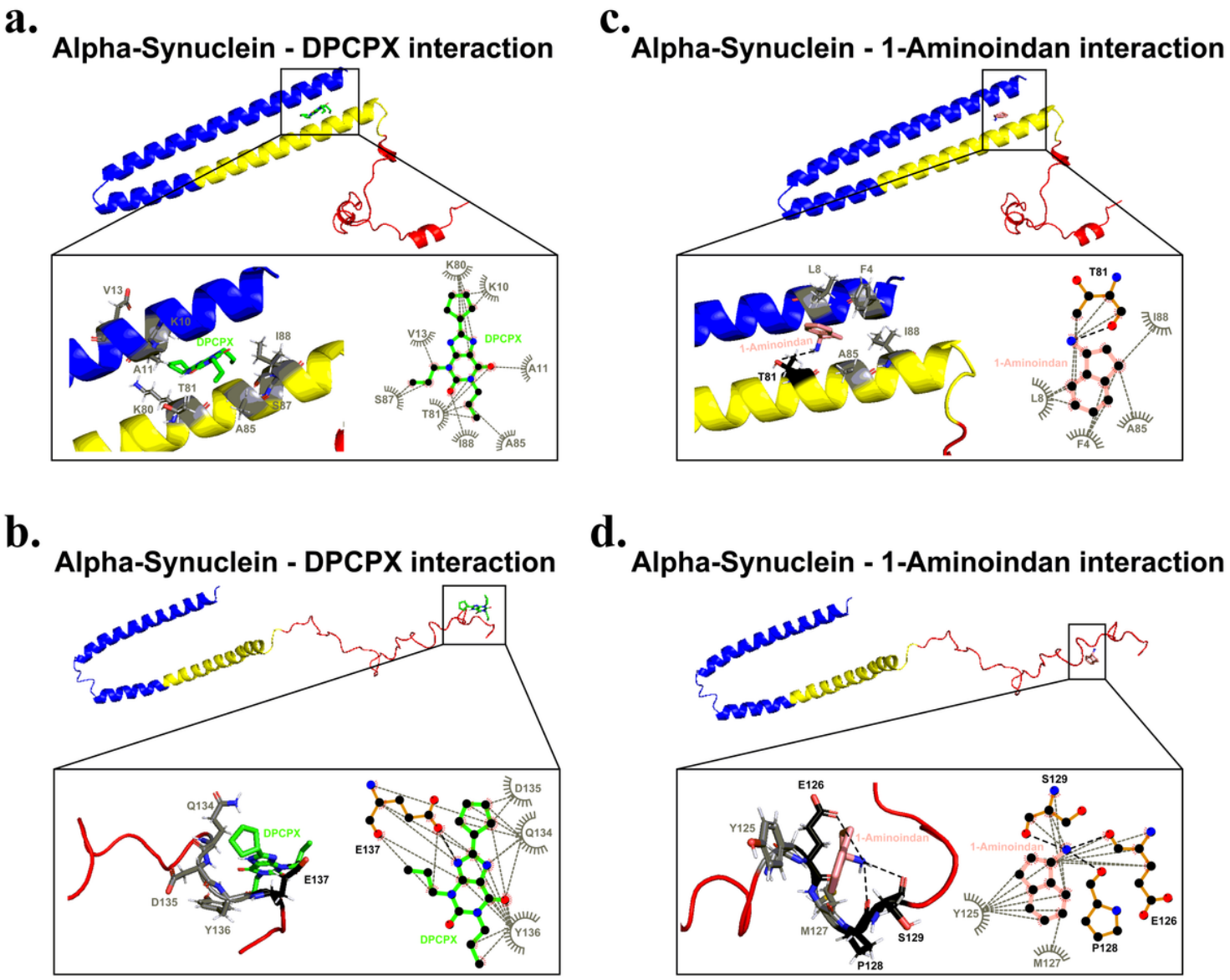

Figure 6

Molecular docking simulation of homology modeled structure α-Synuclein (first panel, a. and c.) and 1XQ8 structure (second panel, b. and d.) bound to DPCPX and 1-aminoindan. In each group the first image is the full 3D representation of the docking of (α-Synuclein blue is the N-terminus, yellow the NAC component and red the C-terminus) bound to DPCPX (a. and b.) and to 1-aminoindan (c. and d.). Below the full 3D representations are shown the magnified binding domains of α-Synuclein and the amino acid residues in both the N- and C- terminus of α-Synuclein that facilitate drug binding. Bold black dashed lines indicate hydrogen bonding. The molecular docking study was performed using Autodock Vina module implemented in PyRx tool. Protein and ligand interactions were analyzed and visualized through Pymol and LigPlot+.

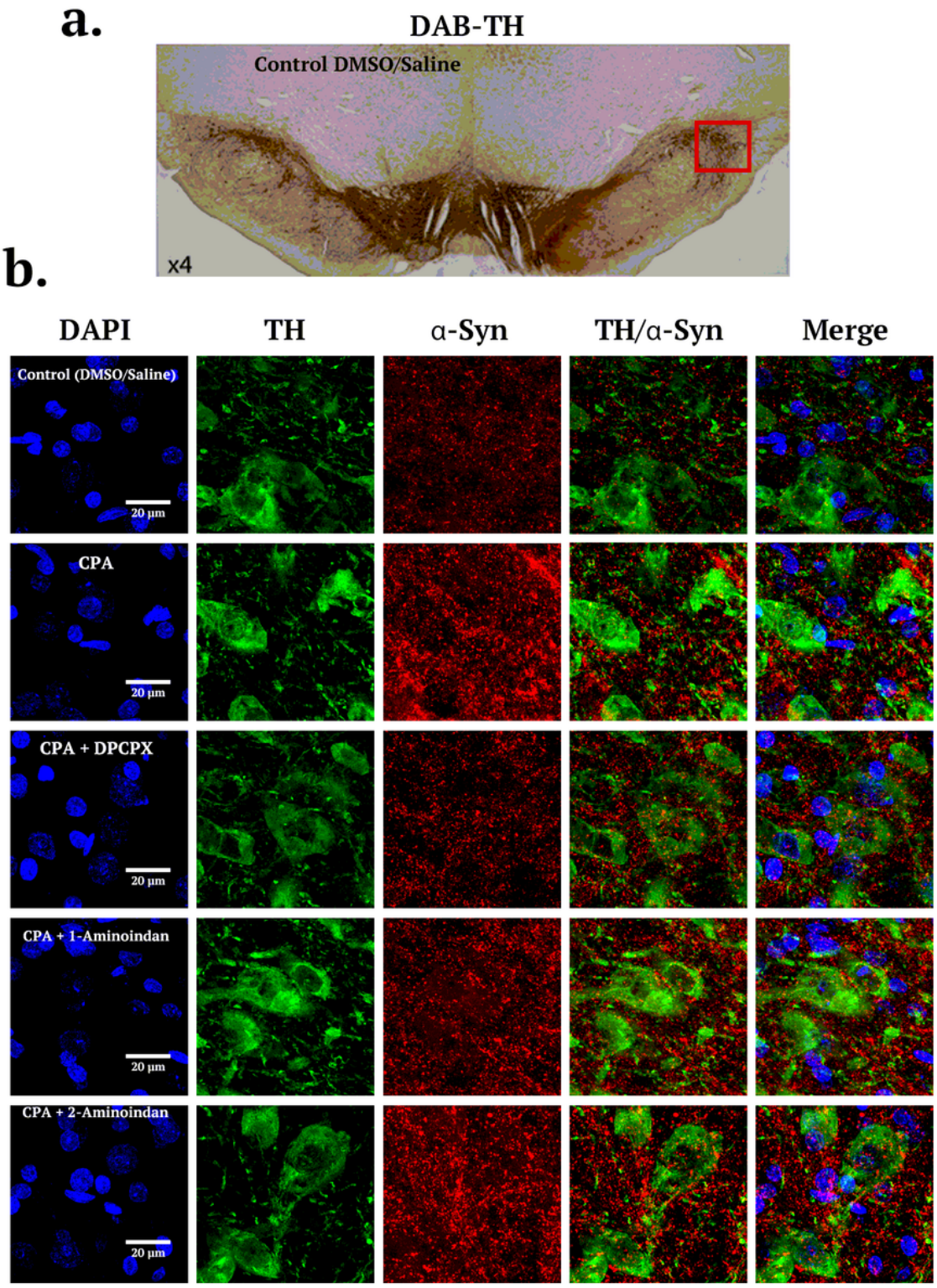

Figure 7

Effects of CPA in absence or presence of DPCPX, 1-aminoindan, and 2-aminoindan on α-Synuclein (α-Syn) expression in the substantia nigra pars compacta. (a.) Immunohistochemical staining of a 40 µm rat nigral brain slice (from a DMSO/Saline control group) labelled with 3,3'-Diaminobenzidine (DAB) and Tyrosine Hydroxylase (TH) taken at 4X magnification with a light microscope. (b.) Representative high magnification confocal images of 40 µm substantia nigra pars compacta region (indicated by square box

in a) taken with 63X oil immersion objective lens. Separate channels and montages of 7-day chronic intraperitoneal injections with 3 mg/kg of the following treatments: Control (DMSO/Saline), CPA, DPCPX + CPA, 1-aminoindan + CPA, and 2-aminoindan + CPA. Slices were probed for DAPI (Blue), Tyrosine Hydroxylase (Green, Alexa Fluor 555), and α-Synuclein (Red, Alexa Fluor 647). CPA alone (second row) or in combination with 2-aminoindan (fifth row) both increased α-Syn expression. Scale bar = 20 μm.

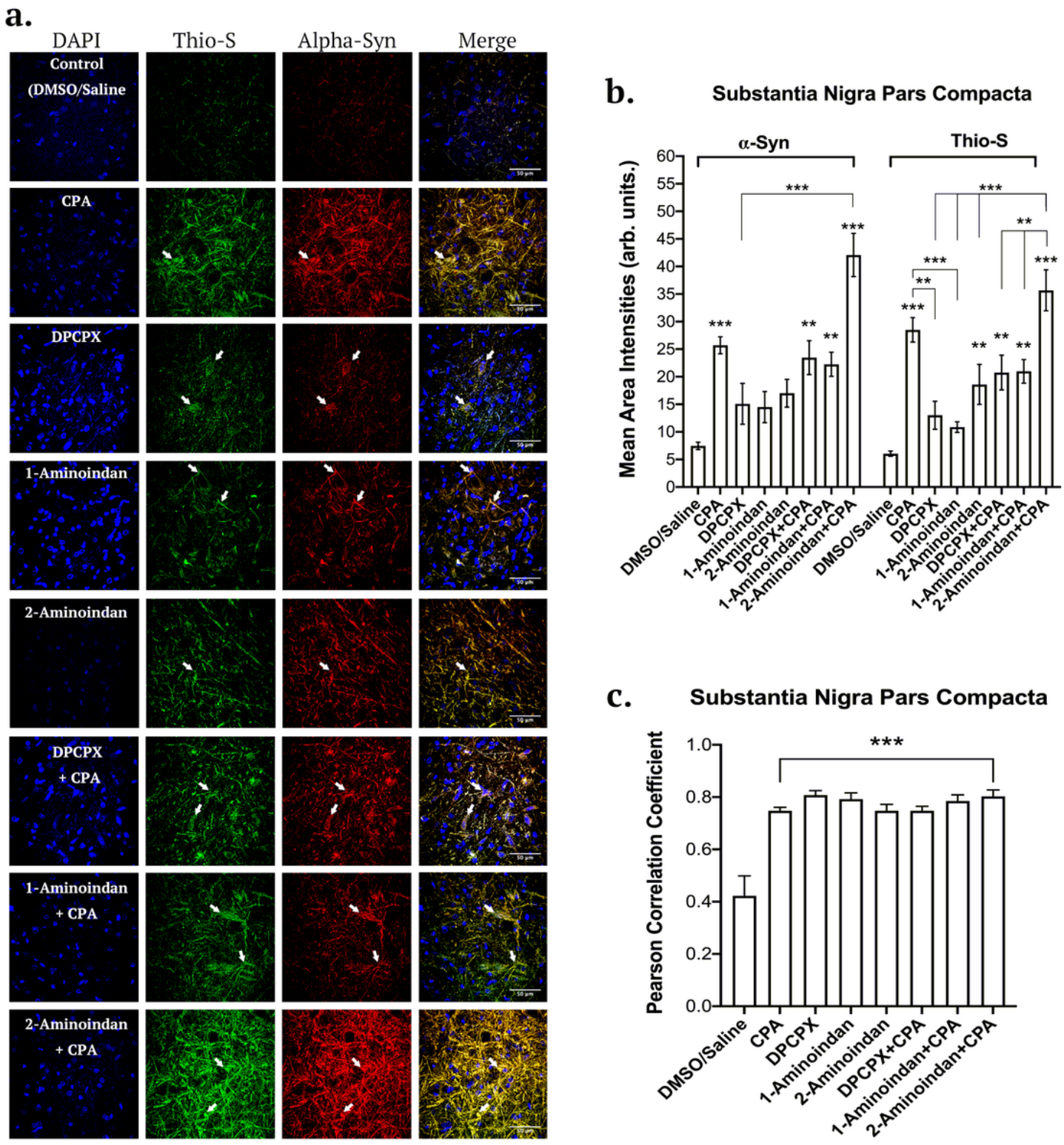

Figure 8

Effects of A1R agonist CPA alone, DPCPX, 1-aminoindan, 2-aminoindan alone or combined with CPA on α-Syn accumulation and aggregation. (a.) Representative confocal microscopy images from 40 μm rat nigral brain slices probed with DAPI, anti-α-Synuclein and Thioflavin-S taken at high magnification with 63X oil immersion objective lens. The various 7-day chronic treatments were as follows: Control (DMSO/Saline), CPA, DPCPX, 1-aminoindan, 2-aminoindan, DPCPX + CPA, 1-aminoindan + CPA, and 2-aminoindan + CPA. Scale bar = 50 μm. (b.) Bar charts showing the mean area intensities of α-Syn and Thioflavin S (Thio-S) from the pars compacta regions of the substantia nigra and the corresponding treatments. Similar areas of 100 by 100 μm regions of interest from the lateral pars compacta of SN were quantified for each slice and normalized by subtracting F0 values of the background (area outside brain slice). Average intensity values in bars represent the mean area fluorescence intensities ± standard error of the mean. The average intensities were obtained from N=4 brain slices from different animals (coronal slices taken at bregma ranges from -5.30 to -5.60). Maximum α-Syn and Thio-S signals were observed in CPA alone and 2-aminoindan + CPA treatments. Neither DPCPX nor 1-aminoindan significantly attenuated the CPA-induced increase in α-Syn and Thio-S signals. (c.) Bar chart showing the Pearson correlation coefficients of α-Syn and Thio-S signals, indicating that all treatments increased colocalization of α-Syn and Thio-S by 2-fold. Average correlation coefficients in bars represent the mean ± standard errors of the mean (N=4 as in b). Significances are denoted as follows: * $p < 0.05$; ** $p < 0.01$; and *** $p < 0.001$.

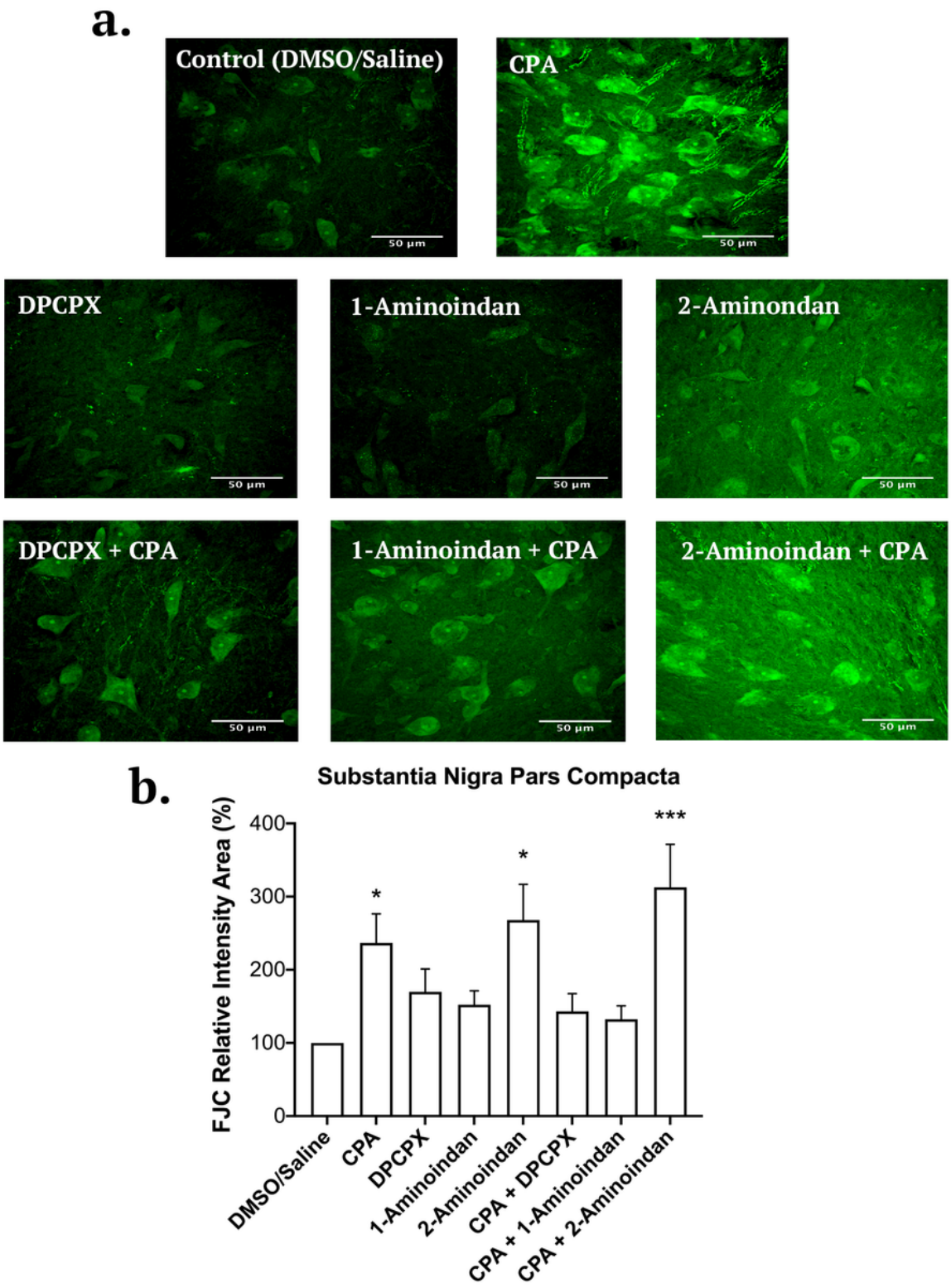

Figure 9

Fluoro-Jade C (FJC) staining of the pars compacta dopaminergic neurons after the 7-day chronic injection treatments. (a.) Representative high magnification confocal microscopy images of the pars compacta region of the substantia nigra after 7-day chronic intraperitoneal injections of 3 mg/kg: Control (DMSO/saline), CPA, DPCPX, 1-aminoindan, 2-aminoindan, DPCPX + CPA, 1-aminoindan + CPA and 2-aminoindan + CPA. Scale bar = 50 µm. CPA alone or in combination with 2-aminoindan increased

neurodegeneration; DPCPX or 1-aminoindan attenuated the CPA-induced neurodegeneration. (b.) Summary bar graph showing relative fluorescence intensity of FJC staining. A 100 by 100 μm regions of interests of degenerating pars compacta neurons were normalized with the control group (100%). Averaged fluorescence values from 4 independent experiments (i.e., 4 different animals per treatment group) are shown as mean ± standard error of the mean. Significances are * $p < 0.05$; ** $p < 0.01$; and *** $p < 0.001$.

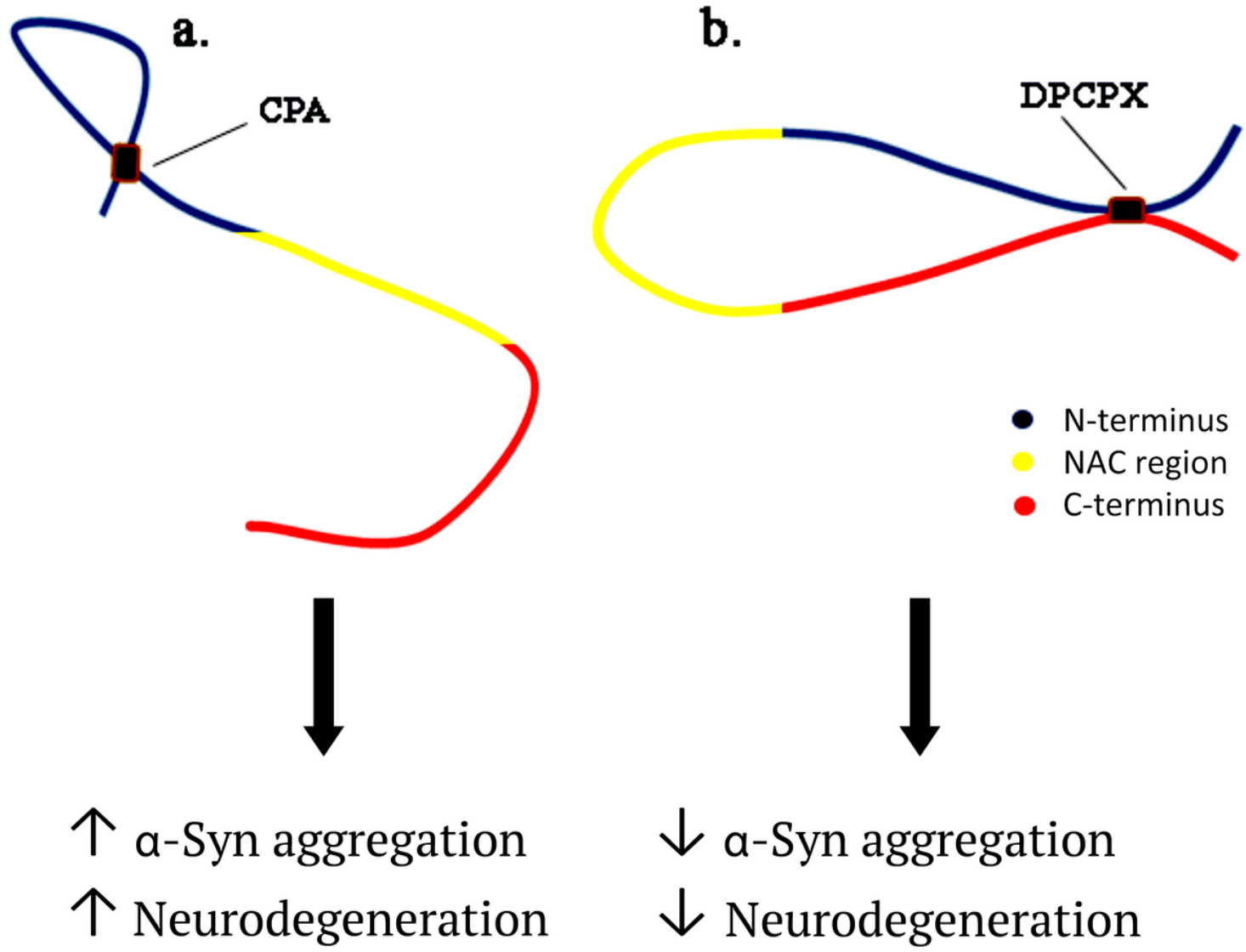

Figure 10

Possible conformations of α-Syn with a. CPA (knot conformation) and b. DPCPX (loop conformation). The knot conformation exposes the NAC region in a manner that promotes α-Syn misfolding, while the loop conformation prevents α-Syn misfolding. Agents acting as A1R inhibitors that also directly bind to the N- and C-terminus of α-Syn may be effective therapeutic options for Parkinson's disease.